

Multipolar Kondo Effect in 1S_0 - 3P_2 Mixture of ^{173}Yb Atoms

Igor Kuzmenko¹, Tetyana Kuzmenko¹, Yshai Avishai^{1,2,4} and Gyu-Boong Jo³

¹Department of Physics,

Ben-Gurion University of the Negev, Beer-Sheva, Israel

²NYU-Shanghai, Pudong, Shanghai, China,

³Department of Physics,

The Hong Kong University of Science and Technology,

Clear Water Bay, Kowloon, Hong Kong, China

⁴ Yukawa Institute for Theoretical Physics,

Kyoto University, Kyoto 606-8502, Japan

Whereas in the familiar Kondo effect the exchange interaction is *dipolar*, there are systems in which the exchange interaction is *multipolar*, as has been realized in a recent experiment. Here we study multipolar Kondo effect in a Fermi gas of cold ^{173}Yb atoms. Making use of different AC polarizabilities of the electronic ground state $\text{Yb}({}^1\text{S}_0)$ and the long-lived metastable state $\text{Yb}^*({}^3\text{P}_2)$, it is suggested that the latter atoms can be localized and serve as a dilute concentration of magnetic impurities while the former ones remain itinerant. The exchange mechanism between the itinerant Yb and the localized Yb^* atoms is analyzed and shown to be antiferromagnetic. The quadrupole and octupole interactions act to enhance the Kondo temperature T_K that is found to be experimentally accessible. The bare exchange Hamiltonian needs to be decomposed into dipole (d), quadrupole (q) and octupole (o) interactions in order to retain its form under renormalization group (RG) analysis, in which the corresponding exchange constants (λ_d , λ_q and λ_o) flow independently. Numerical solution of the RG scaling equations reveals a few finite fixed points. Arguments are presented that the Fermi liquid fixed point at low temperature is unstable, indicating that the impurity is over-screened, which suggests a non-Fermi liquid phase. The impurity contributions to the specific heat, entropy and the magnetic susceptibility are calculated in the weak coupling regime ($T \gg T_K$), and are compared with the analogous results obtained for the standard case of dipolar exchange interaction (the $s-d$ Hamiltonian).

PACS numbers: 31.25.-v,32.80.Pj,72.15.Qm

I. INTRODUCTION

Background In its most elementary form, the (single channel) Kondo model describes the physics of a magnetic impurity (of spin operator \mathbf{S}), immersed in a host metal with a single continuous band of noninteracting electrons (of spin operator \mathbf{s} , with $s = \frac{1}{2}\hbar$)¹⁻⁴. The impurity and the band electrons are coupled via an antiferromagnetic exchange interaction $J\mathbf{s} \cdot \mathbf{S}$ of strength $J > 0$. The corresponding Hamiltonian H_{s-d} has an SU(2) symmetry. The Kondo model can naturally be generalized into the Coqblin-Schrieffer model whose Hamiltonian H_{C-S} has an SU(N) symmetry⁴⁻⁷. Renormalization group (RG) analysis shows that the respective low energy fixed point in either model is stable and that the corresponding fixed point Hamiltonian describes regular or singular Fermi liquid (FL), in which the impurity is fully or under screened.

A seminal paper by Nozières and Blandin (NB) back in 1980, discusses the fixed points of H_{s-d} under the assumption that a few electron channels participate in the impurity screening⁸. More precisely, suppose that by some mechanism, there are N independent electron channels contributing to screening. Then, under favourable conditions on the corresponding exchange constants, together with the (hereafter referred as NB inequality) $N > 2S$, the impurity is *over-screened*. The Hamiltonian of such over-screened Kondo system flows at low temperature to a new fixed point in which it displays a

non-Fermi liquid (NFL) behaviour. Searching for an experimental manifestation of over-screened Kondo effect (KE) in solid state systems was notoriously frustrating, but eventually it was demonstrated in a specifically designed quantum-dot system⁹.

Another route to over-screening in the Kondo effect is *single channel over-screening by large spin Fermi-sea*¹⁰. It is expected to occur when a magnetic impurity is immersed in a host Fermi-sea with a continuous band of noninteracting fermions of spin operator \mathbf{s} , with $s > \frac{1}{2}\hbar$. This system is shown to be equivalent to that with $N(s)$ independent electron channels where

$$N(s) = \frac{2}{3} s(s+1)(2s+1). \quad (1)$$

Since $N(s)$ is a cubic function of s , (for example $N(\frac{5}{2}) = 35$), the NB inequality $N > 2S$ (that is a necessary but not sufficient condition for over-screening) can easily be satisfied. While it is hard (albeit possible) to perceive its realization in solid state systems, the revelation and the possible control of a gas composed of cold fermionic atoms within a periodic optical lattice potential turned this scenario to be realistic also outside the realm of solid-state systems^{11,12}. Indeed, we have recently suggested a general framework for a pertinent experiment to test this scenario of over-screening and analyzed the conditions and parameter range for its realization¹³. It can be performed in a few laboratories that specialize in controlling cold fermionic atoms.

In both cases (multi-channel and/or large spin over screening), the corresponding Hamiltonian has an $SU(2)$ symmetry, and the exchange interaction is *dipolar*. An extension of the $SU(2)$ multi-channel over-screening scenario into over-screened multi-channel $SU(N)$ Kondo model is discussed in Ref.¹⁴.

In the present work we focus on an experimentally accessible cold atom system and examine the concept of large spin Kondo over-screening beyond $SU(2)$, in case where the exchange interaction is *multipolar*. This is motivated by a recent experiment where a multipolar KE is realized in solid state system¹². For the cold atom arena, a concrete experimental candidate system is that of fermionic alkali-earth-like isotopes such as ^{173}Yb atoms^{15,16,18,19}. The underlying idea is to localize an ^{173}Yb atom in its long lived excited $^3\text{P}_2$ state with atomic spin $F = \frac{3}{2}$, in a Fermi sea of non (or weakly)-interacting itinerant ^{173}Yb atoms in their ground state $^1\text{S}_0$ with atomic spin $I = \frac{5}{2}$. For that purpose, it should be demonstrated that an antiferromagnetic exchange interaction exists between the impurity $\text{Yb}^*(^3\text{P}_2)$ and the itinerant $\text{Yb}(^1\text{S}_0)$ atoms. Intuitively, in that case we might expect an over-screening by large spin scenario, since the angular momentum of the itinerant atoms is larger than that of the impurity atom ($I = \frac{5}{2} > F = \frac{3}{2}$). However, quantitative analysis turns out to be extremely complicated, due to several factors. First, elucidation and calculation of the exchange interaction is rather involved, and requires sophisticated multiple expansions to handle the pertinent angular momentum algebra. Second, identifying and constructing the explicit form of the exchange term is rather tedious, and, unfortunately, the pertinent Kondo Hamiltonian does not have a definite symmetry. Third, in order to identify the NFL fixed points, perturbative RG calculations within the poor-man scaling procedure must go at least up to third order and the relevant expressions are long and involve multiple summations on angular momentum quantum numbers. Finally, elucidating the NFL physics requires the use of non-perturbative techniques (Bethe ansatz or conformal field theory) which are still not developed for this class of Hamiltonians.

It is worthwhile stressing at this early stage a central point distinguishing multipolar from an $SU(2)$ over-screening resulting from our analysis: If the spin F of the impurity and the spin I of itinerant fermions satisfy the inequalities

$$F \geq 3/2, \quad I \geq 3/2, \quad N(I) > 2S,$$

the NB fixed point $j^* = 1/N(I)$ is unstable. The stable fixed points exposed here are distinct from the NB fixed point, and correspond to different NFL phases. The reason is that in the process of carrying out Schrieffer-Wolf transformations, one usually restricts oneself to second order perturbation theory. However, when quadrupole, octupole and higher exchange interactions are present, new interactions are generated within the Schrieffer-Wolf procedure. At high temperature these interactions are weaker than the lowest order (dipole) interaction. But

at low temperature, these interactions turn the NB fixed point to be unstable.

Organization: The paper is organized as follows: In section II the question of experimental realization is addressed. Specifically, we substantiate the feasibility of fabricating a system consisting of a Fermi gas of ^{173}Yb atoms in their ground state (electronic configuration $^1\text{S}_0$) and a small concentration of ^{173}Yb atoms in their long lived excited state (electronic configuration $^3\text{P}_2$) trapped in a suitably designed optical potential. The rest of the paper is devoted to theoretical analysis. Exchange interaction between $^{173}\text{Yb}(^1\text{S}_0)$ and $^{173}\text{Yb}^*(^3\text{P}_2)$ atoms is analyzed in section III, while the Kondo Hamiltonian H_K is derived in section IV. The main technical endeavours are related to the decomposition of H_K into 2^n poles components ($n = 1, 2, 3$), and the numerical estimates of the pertinent coupling constants. In section V the perturbative RG calculations pertaining to H_K are detailed up to second order. Although the derivation of these corrections is rather technical, we find it useful to present it within the main text because it starts from the standard diagrams of poor-man's scaling analysis, and the analysis that enables us to overcome the complexities stemming from the relevant spin algebra is quite instructive. At the end of this section we write down and solve the relevant scaling equations (up to second order). The solutions enable us to elucidate the Kondo temperature T_K , as explained in section VI. However, to find stable fixed points that are candidates for NFL behaviour, one must expand the perturbative RG calculations up to third order. These calculations are carried out in section VII. Despite its highly technical nature, we include it in the main text, for the same reasons as for section V. The most significant result that emerges is a list of seven possible fixed points. Yet, further stability analysis is required in order to sort out the stable ones, by linearizing the RG equations and identifying relevant and irrelevant exponents. At the end of this procedure, only three stable points are left. Analysis of the relation between the fixed points and the interaction parameters is carried out in section VIII, and the claim that the infinite fixed point in the strong coupling limit is unstable is detailed in section IX.

In section X we derive (in the weak coupling regime $T > T_K$) expressions for the impurity contributions to a few thermodynamic observables related to this system, and compare them with the corresponding quantities for the standard KE based on the $s-d$ exchange Hamiltonian. These include the impurity contribution to the specific heat, entropy and magnetic susceptibility. A short summary listing our main achievements is presented in section XI. Numerous technical issues are discussed in the Appendices.

II. EXPERIMENTAL FEASIBILITY

Recent development of producing degenerate Bose and Fermi gases of alkaline-earth-like atoms has attracted a

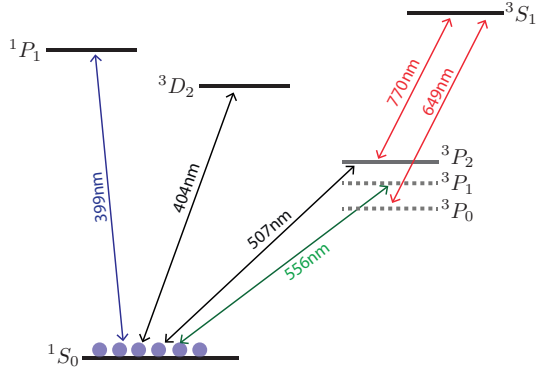


FIG. 1: (color online) The electronic level structure of ^{173}Yb atoms. A small portion of the atoms are optically pumped into the $^3\text{P}_2$ excited state via a resonant $^1\text{S}_0$ - $^3\text{P}_2$ transition or an intermediate $^1\text{S}_0$ - $^3\text{D}_2$ transition.

great deal of interests in utilizing such atoms for the study of many-body physics (in the context of quantum simulation)^{20–22} and the realization of quantum computation^{23,24}. The enlarged $SU(N)$ spin symmetry for the fermionic isotopes of alkaline-earth-like atoms expands our capability in exploring large spin physics in low dimensions²⁰ and a two-orbital Fermi gas with $SU(N)$ interactions^{21,22,25} in which the interactions can be tuned by the orbital Feshbach resonance¹⁶. In addition, a narrow optical transition between the singlet and the triplet state enables to realize a spin-orbit coupled Fermi gas with minimal heating^{26–30}, and a long-lived triplet state holds the promise in studying the KE¹⁷. It has recently also been demonstrated that in such a systems, the Kondo temperature can be increased due to the spin-exchange interaction and the confinement-induced resonance effect¹⁸.

More concretely, making use of different AC polarizabilities of the ground state and the metastable state, the latters can be localized and serve as local moments. Then, KE is expected to occur due to an exchange interaction between the atoms in the ground state $^1\text{S}_0$ and the atoms in the metastable $^3\text{P}_J$ state. Such scenario, pertaining to spin-exchange interactions between $^1\text{S}_0$ and $^3\text{P}_0$ states has been explored in our previous work where it is shown to realize an $SU(6)$ Coqblin-Schrieffer model³¹.

Here, we consider ytterbium atoms in the metastable $^3\text{P}_2$ (Yb^*) state as magnetic impurities for itinerant ground-state $^1\text{S}_0$ (Yb) atoms. We begin with a Fermi gas of the ground-state ^{173}Yb atoms. Subsequently, a small portion, a few % of the ground state $^1\text{S}_0$ atoms will be directly transferred to $^3\text{P}_2$ using a narrow line-width 507 nm optical transition $^1\text{S}_0$ - $^3\text{P}_2$ ³². Alternatively, the ground state atoms may be pumped into the state $^3\text{D}_2$ with a 404 nm light and then spontaneously decay to the $^3\text{P}_2$ state³³. During the pumping process, a three-dimensional optical lattice potential may be applied to suppress the recoil kick in the Lamb Dicke regime.

To realize the Kondo model in a mixture of $^1\text{S}_0$ - $^3\text{P}_2$

atoms, it is critical to minimize the anisotropy of the trap potential for the localized $^3\text{P}_2$ atoms whose atomic polarizability $\alpha_{|m_J|}$ is $|m_J|$ -dependent with the total angular momentum $J=2$. Such anisotropic polarizability would lift the degeneracy of the Kondo state of localized $^3\text{P}_2$ atoms. For this reason, we propose to use the trapping light at the double-magic wavelength $\lambda_0 \simeq 546$ nm which results³³ $\alpha_{|m_J|} = \alpha_e(\lambda_0)$ for $|m_J| \leq 2$. After preparing a mixture of $^1\text{S}_0$ - $^3\text{P}_2$ atoms, a three-dimensional optical lattice generated by double-magic wavelength lights is adiabatically switched on in such a way that the Fermi energy of $^1\text{S}_0$ atoms is larger than the lattice depth while the low-density $^3\text{P}_2$ atoms are localized by the lattice potential.

In the proposed experiment, ytterbium atoms in different orbitals, Yb and Yb^* atoms, can be selectively detected to extract the thermodynamic quantities that will be discussed later. The Yb atom in the $^1\text{S}_0$ state are imaged using the 399 nm $^1\text{S}_0$ - $^1\text{P}_1$ transition. To image Yb^* atoms, we first blast Yb atoms with 399 nm light followed by optical pumping Yb^* atoms into the $^3\text{P}_1$ state with 770 nm and 649 nm lights (see Fig. 1). The pumped atoms in the $^3\text{P}_1$ state then decay to the $^1\text{S}_0$ state that can be imaged by 399 nm light³².

III. EXCHANGE INTERACTION

Section III main points: In subsections III A and III B we introduced multiple operators: A 2^n pole operator is an expression involving n spin operators, with appropriate coefficients. These operators, explicitly calculated in this section, are the building blocks of the exchange interaction of the multipolar Kondo Hamiltonian to be introduced in the next section. Finally, in subsection III C the basic mechanism for exchange interaction between two atoms $^{173}\text{Yb}(^3\text{P}_2)$ - $^{173}\text{Yb}(^1\text{S}_0)$ is explained. It is similar but not identical with the exchange interaction between two atoms $^{173}\text{Yb}(^3\text{P}_0)$ - $^{173}\text{Yb}(^1\text{S}_0)$ discussed in Ref.³¹ because here, the total electronic spin of one of the atoms is not zero. More concretely, this section introduces the main ingredients required for the construction of the Kondo Hamiltonian (that is carried out in the next section). The basic notations and numerous algebraic manipulations pertaining to the geometry of multipolar interactions are specified, and the relevant exchange interactions are derived and analyzed.

A. Notations

In this subsection we introduce the definitions and expressions for the 2^n poles required for the representation of the Kondo Hamiltonian in terms of multiple expansion. These 2^n poles result from the spin content of the underlying atomic system.

We consider exchange interaction of itinerant atoms (which are ^{173}Yb atoms in the ground $^1\text{S}_0$ state with atomic spin $I = \frac{5}{2}$), and localized impurities (which are

the same ^{173}Yb atoms in the long lived excited $^3\text{P}_2$ state with atomic spin $F = \frac{3}{2}$). Note that I is contributed solely from the nuclear spin while F is the sum of electronic and nuclear spins. An atom with total angular momentum $F = \frac{3}{2}$ has nontrivial dipole, quadrupole and octupole magnetic momenta. They are denoted here as

$$\hat{F}^\alpha, \quad \hat{F}^{\alpha, \alpha'}, \quad \hat{F}^{\alpha, \alpha', \alpha''},$$

where α, α' and α'' are Cartesian indices. An atom with total angular momentum $I = \frac{5}{2}$ has nontrivial dipole, quadrupole, octupole, 16-pole and 32-pole magnetic momenta, denoted here as

$$\begin{aligned} \hat{I}^{\alpha_1}, \quad & \hat{I}^{\alpha_1, \alpha_2}, \quad \hat{I}^{\alpha_1, \alpha_2, \alpha_3}, \\ \hat{I}^{\alpha_1, \alpha_2, \alpha_3, \alpha_4}, \quad & \hat{I}^{\alpha_1, \alpha_2, \alpha_3, \alpha_4, \alpha_5}. \end{aligned}$$

When an expression applies for both itinerant atoms and impurities, we use the notations $\hat{S}^\alpha, \hat{S}^{\alpha, \alpha''}, \hat{S}^{\alpha, \alpha', \alpha''}$ for the dipole, quadrupole and octupole angular momenta. Here \hat{S} denotes the operators \hat{F} or \hat{I} .

B. Explicit expressions for 2^n -Pole Momenta

The magnetic dipole operator is collinear with the vector of its spin (more precisely its total angular momentum) operator. When a particle has spin S , the vector \mathbf{S} of the spin matrices (generators of the $2S+1$ -dimensional representation of the SU(2) group) are,

$$S_{s, s'}^z = s \delta_{s, s'}, \quad (2a)$$

$$S_{s, s'}^+ = \mathcal{L}(S, s) \delta_{s, s'+1}, \quad (2b)$$

$$S_{s, s'}^- = \mathcal{L}(S, s') \delta_{s', s+1}, \quad (2c)$$

where s, s' are magnetic quantum numbers such that $|s| \leq S$, and

$$\mathcal{L}(S, s) = \sqrt{(S+s)(S-s+1)}.$$

Next, the quadrupole moment operators are represented by symmetric traceless matrices $S^{\alpha, \alpha'}$ ($\alpha, \alpha' = x, y, z$ are Cartesian indices) defined as,

$$\hat{S}^{\alpha, \alpha'} = \{\hat{S}^\alpha, \hat{S}^{\alpha'}\} - \frac{2}{3} \hat{\mathbf{S}}^2 \delta^{\alpha, \alpha'}, \quad (3)$$

where

$$\{\hat{S}^\alpha, \hat{S}^{\alpha'}\} = \hat{S}^\alpha \hat{S}^{\alpha'} + \hat{S}^{\alpha'} \hat{S}^\alpha.$$

The quadrupole operators satisfy the following equalities,

$$\hat{S}^{\alpha, \alpha'} = \hat{S}^{\alpha', \alpha}, \quad \sum_\alpha \hat{S}^{\alpha, \alpha} = 0. \quad (4)$$

Continuing this analysis, the octupole moment operators are represented by matrices,

$$\begin{aligned} \hat{S}^{\alpha, \alpha', \alpha''} = & \{\hat{S}^\alpha, \hat{S}^{\alpha'}, \hat{S}^{\alpha''}\} - \frac{1}{5} (3 \hat{\mathbf{S}}^2 - 1) \times \\ & \times \sum_{\alpha_1, \alpha'_1, \alpha''_1} P_{\alpha_1, \alpha'_1, \alpha''_1}^{\alpha, \alpha', \alpha''} \delta^{\alpha_1, \alpha'_1} \hat{S}^{\alpha''_1}. \end{aligned} \quad (5)$$

Here the symbol $P_{\alpha_1, \alpha'_1, \alpha''_1}^{\alpha, \alpha', \alpha''}$ denotes permutation of the indices $\alpha, \alpha', \alpha''$,

$$\begin{aligned} P_{\alpha_1, \alpha'_1, \alpha''_1}^{\alpha, \alpha', \alpha''} = & \delta_{\alpha, \alpha_1} P_{\alpha'_1, \alpha''_1}^{\alpha', \alpha''} + \delta_{\alpha, \alpha'_1} P_{\alpha''_1, \alpha_1}^{\alpha', \alpha''} + \\ & + \delta_{\alpha, \alpha''_1} P_{\alpha_1, \alpha'_1}^{\alpha', \alpha''}, \end{aligned} \quad (6)$$

the symbol $P_{\alpha_1, \alpha'_1}^{\alpha, \alpha'}$ denotes permutation of the indices α, α' ,

$$P_{\alpha_1, \alpha'_1}^{\alpha, \alpha'} = \delta_{\alpha, \alpha_1} \delta_{\alpha', \alpha'_1} + \delta_{\alpha, \alpha'_1} \delta_{\alpha', \alpha_1}. \quad (7)$$

The symbol $\{\hat{S}^\alpha, \hat{S}^{\alpha'}, \hat{S}^{\alpha''}\}$ is fully symmetric product of $\hat{S}^\alpha, \hat{S}^{\alpha'}$ and $\hat{S}^{\alpha''}$,

$$\{\hat{S}^{\alpha_1}, \hat{S}^{\alpha_2}, \hat{S}^{\alpha_3}\} = \sum_{\{\alpha'\}_3} P_{\alpha'_1, \alpha'_2, \alpha'_3}^{\alpha_1, \alpha_2, \alpha_3} \hat{S}^{\alpha'_1} \hat{S}^{\alpha'_2} \hat{S}^{\alpha'_3},$$

where $\{\alpha'\}_3 = \{\alpha'_1, \alpha'_2, \alpha'_3\}$. The octupole operators are symmetric with all the indices,

$$\hat{S}^{\alpha, \alpha', \alpha''} = \hat{S}^{\alpha', \alpha, \alpha''} = \hat{S}^{\alpha, \alpha'', \alpha'}.$$

Moreover, they are constructed in such a way that the trace over any two indices vanishes that is,

$$\sum_{\alpha'} \hat{S}^{\alpha, \alpha', \alpha'} = 0.$$

C. Exchange Interaction

When the distance between itinerant $\text{Yb}(^1\text{S}_0)$ and impurity $\text{Yb}^*(^3\text{P}_2)$ atoms is of the same order as the atomic size R_0 , there is an *indirect exchange interaction* between them³¹. Heuristically it is described in two steps [see Fig. 2 for illustration]: 1) A $6p$ electron tunnels from the excited $\text{Yb}(^3\text{P}_2)$ atom to the ground state $\text{Yb}(^1\text{S}_0)$ atom. As a result, we have two ions with parallel electronic orbital angular momenta. 2) Then, one electron from the $6s$ orbital tunnels from the negatively charged ion to the $6s$ orbital of the positively charged ion. The net outcome is that the atoms “exchange their identity” specified by their electronic quantum states: one atom transforms from the ground state to the excited state, whereas the other atom transforms from the excited state to the ground state. The detailed calculations of the pertinent exchange interaction is relegated to the Appendix B (see also Ref.³¹). They employ two-particle wave functions describing the motion of two atoms in the optical potential, taking into account the atom-atom interaction. For short distance between the atoms, (where the exchange interaction is essential), the two-atom wave function is determined mainly by the inter-atomic van der Waals potential³¹. The exchange interaction strength is given by,

$$\lambda_0 = \sqrt{3} \Gamma^2 \left(\frac{3}{2} \right) \int_{r_0}^{\infty} g(R) R^2 dR, \quad (8)$$

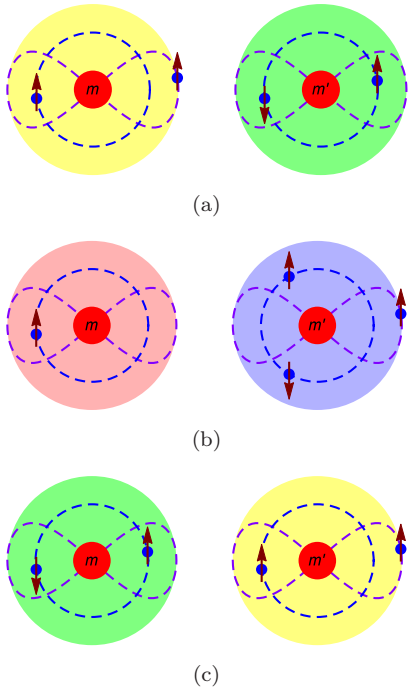


FIG. 2: (color line) Illustration of exchange interaction between ytterbium atoms. Panel (a): Initial quantum state - the first atom is in the meta-stable state (light yellow disk) and the second one is in the ground state (light green disk); panel (b): virtual state - the first atom is positively ionized (light red disk), and the second one is negatively charged (light blue disk); panel (c): final state - the first atom is in the ground state and the other one is in the meta-stable state. For all the panels, arrows denote the electronic spin, m or m' is nuclear spin of the first or second atom.

where L is the size of the trapping box of the $\text{Yb}({}^1\text{S}_0)$ atoms. $r_0 = 3.6673 \text{ \AA}$ is found from the condition $W(r_0) = 0$, where $W(R)$ is the van der Waals potential between an itinerant atom and the impurity. We approximate the van der Waals interaction by the Lennard-Jones potential as³⁶,

$$W(R) = -\frac{C_6}{R^6} - \frac{C_8}{R^8} + \frac{C_{12}}{R^{12}}. \quad (9)$$

Here $C_6 = 2.649 \cdot 10^3 E_h a_B^6$, $C_8 = 3.21097 \cdot 10^5 E_h a_B^8$ and $C_{12} = 1.41808 \cdot 10^9 E_h a_B^{12}$, where $E_h = 27.2114 \text{ eV}$ and $a_B = 0.529177 \text{ \AA}$.

The function $g(R)$ is [see Appendix B for details],

$$g(R) = \frac{t_s(R) t_p(R)}{3 \Delta \epsilon} \mathfrak{R}(R). \quad (10)$$

Here t_s and $t_p = \frac{1}{3}(t_0 + 2t_1)$ are tunneling rates for the 6s and 6p electrons³¹,

$$t_\nu(R) = t_\nu^{(0)} \left(\frac{R}{r_0} \right)^{\frac{2}{\beta_\nu} + \frac{1}{2}} e^{-\kappa_\nu(R-r_0)}, \quad (11)$$

where $\nu = \text{s, p}$.

$$t_s^{(0)} = 1.09 \text{ eV}, \quad t_p^{(0)} = 1.82 \text{ eV}.$$

The parameters κ_ν and β_ν are

$$\begin{aligned} \kappa_s &= 1.28122 \text{ \AA}^{-1}, & \beta_s &= 0.677994, \\ \kappa_p &= 1.00005 \text{ \AA}^{-1}, & \beta_p &= 0.529206. \end{aligned}$$

$\Delta\epsilon = \varepsilon_{\text{ion}} + \varepsilon_{\text{ea}} - \epsilon_x = 4.1104 \text{ eV}$ is the energy which should be paid to get positively and negatively charged ions from two neutral atoms, where $\varepsilon_{\text{ion}} = 6.2542 \text{ eV}$ is the ionization energy³⁷, $\varepsilon_{\text{ea}} = 0.3 \text{ eV}$ is the electron affinity³⁸ and $\epsilon_x = 2.4438 \text{ eV}$ is the excitation energy of the ${}^3\text{P}_2$ state³⁷. The function $\mathfrak{R}(R)$ encodes the deformation of the wave function of the itinerant fermions at short distance from the impurity where the van der Waals interaction is significant³¹,

$$\mathfrak{R}(R) = \frac{8c}{R^2 K(R)} \left\{ 1 + \left(\frac{a_w - \bar{a}}{\bar{a}} \right)^2 \right\}.$$

Here $K(R) = \frac{1}{\hbar} \sqrt{-MW(R)}$, $a_w = 20.9973 \text{ \AA}$, $\bar{a} = 42.9984 \text{ \AA}$ and $c = 89.9569 \text{ \AA}$.

IV. THE KONDO HAMILTONIAN

Section IV main points: The simple form of the exchange Hamiltonian [see below Eq. (12)], involves a single bare coupling constant λ_0 , but in this form, it does not keep its structure under the RG transformation (introduced in the next section). It is then necessary to decompose the bare Hamiltonian (12) into a sum of terms with *different multi-polarities*, H_d , H_q , H_o as was carried out above. The prefactors relating the bare coefficients λ_d , λ_q , λ_o to λ_0 are explicitly calculated above. However, as will be shown in the next section, λ_d , λ_q , λ_o are renormalized *differently*.

We start by writing down the bare Hamiltonian describing the scattering of itinerant ${}^{173}\text{Yb}({}^1\text{S}_0)$ and localized ${}^{173}\text{Yb}({}^3\text{P}_2)$ atoms. Recall that the itinerant atom is in the ground state with total atomic spin $I = \frac{5}{2}$ (which is the nuclear spin), and the trapped atom is in the long lived excited state with its total atomic spin being $F = \frac{3}{2}$. The latter serves as a localized impurity described by the Hubbard operators $X^{f=F_z, f'=F'_z}$,

$$X^{f, f'} = |F, f\rangle \langle F, f'|,$$

where $|F, f\rangle$ is the wave function of the localized impurity with total spin F and magnetic quantum number f . The itinerant atoms form Fermi gas. The wave functions of the itinerant atoms are derived in Appendix A. They are described by the harmonic quantum number n and the (nuclear) magnetic quantum number i . The interaction between the atoms, consisting of potential scattering and exchange terms, reads³¹,

$$\begin{aligned} H_K = & \frac{\lambda_0 k_F}{a_g^2} \sum_j \sum_{f, f'} \sum_{i, i'} \sum_{n, n'} C_{J, j; I, i}^{F, f} C_{J, j; I, i'}^{F, f'} \times \\ & \times X^{f, f'} c_{n', i'}^\dagger c_{n, i}, \end{aligned} \quad (12)$$

were

$$k_F = \frac{\sqrt{2M\epsilon_F}}{\hbar},$$

where ϵ_F is the Fermi energy. $C_{J,j;I,i}^{F,f}$ are the Clebsch-Gordan coefficients. The coupling λ_0 is given by eq. (8). $c_{n,i}$ and $c_{n,i}^\dagger$ are creation and annihilation operators of the Yb(1S_0) atoms with harmonic quantum number n and magnetic quantum number i . The integer j is an electronic magnetic quantum number of the Yb atom in the 3P_2 state, $|j| \leq J$, where $J = 2$ is the total electronic angular momentum. The harmonic length a_g and frequency Ω_g of the trapped Yb($1S_0$) atoms are given by eq. (A21) in Appendix A.

The Hamiltonian (12) conserves the z component of the total angular momentum that is,

$$i + f' = i' + f.$$

The selection rules for the Hamiltonian (12) are,

$$\Delta f = f - f' = 0, \pm 1, \pm 2, \pm 3. \quad (13)$$

We shall now rewrite this *same Hamiltonian* as a sum of terms representing potential, dipole, quadrupole and octupole interactions,

$$H_K = H_p + H_d + H_q + H_o. \quad (14)$$

The precise expressions for these multipolar components are given in the next subsection. As will be evident from the discussion below, this form of the Hamiltonian is more complicated than its initial form (12). The reason for using the equivalent form (14) is that the form (12) of the Hamiltonian *changes under poor-man's scaling procedure*, and that violates the spirit of the RG formalism. We need to express the Hamiltonian in such a way that its structure is unchanged under the poor-man's scaling procedure, albeit the coupling constants renormalize. As we shall show below, this is indeed the case once we use the form (14).

A. Bare exchange coefficients and structure of multiple terms

The four terms in the decomposition (14) involve four exchange coefficients $\lambda_{p,d,q,o}$, each one being proportional to λ_0 . The proportionality constants are just simple geometric factors to be written down below. Before that, let us specify the structure of the four parts of H_K .

The first term on the right hand side of eq. (14), H_p , is potential scattering,

$$H_p = \frac{\lambda_p k_F}{a_g^2} \sum_f \sum_i \sum_{n,n'} X^{f,f} c_{n',i}^\dagger c_{n,i}. \quad (15)$$

The second term on the right hand side of eq. (14), H_d , is dipole interaction,

$$H_d = \frac{\lambda_d k_F}{a_g^2} \sum_\alpha \sum_{f,f'} \sum_{i,i'} \sum_{n,n'} F_{f,f'}^\alpha I_{i',i}^\alpha X^{f,f'} c_{n',i'}^\dagger c_{n,i}, \quad (16)$$

where $\hat{\mathbf{F}} = (\hat{F}^x, \hat{F}^y, \hat{F}^z)$ and $\hat{\mathbf{I}} = (\hat{I}^x, \hat{I}^y, \hat{I}^z)$ are vectors of the spin- F and spin- I matrices and λ_d is a coupling constant of the dipole interaction. The third term on the right hand side of eq. (14), H_q , is quadrupole interaction,

$$H_q = \frac{\lambda_q k_F}{a_g^2} \sum_{\alpha,\alpha'} \sum_{f,f'} \sum_{i,i'} \sum_{n,n'} F_{f,f'}^{\alpha,\alpha'} I_{i',i}^{\alpha',\alpha} \times X^{f,f'} c_{n',i'}^\dagger c_{n,i}, \quad (17)$$

where $\hat{F}^{\alpha,\alpha'}$ or $\hat{I}^{\alpha,\alpha'}$ are the quadrupole matrices of the particle with spin F or I , λ_q is a coupling of the quadrupole interaction. Finally, the fourth term on the right hand side of eq. (14), H_o , is octupole interaction,

$$H_o = \frac{\lambda_o k_F}{a_g^2} \sum_{\alpha,\alpha',\alpha''} \sum_{f,f'} \sum_{i,i'} \sum_{n,n'} F_{f,f'}^{\alpha,\alpha',\alpha''} I_{i',i}^{\alpha'',\alpha',\alpha} \times X^{f,f'} c_{n',i'}^\dagger c_{n,i}, \quad (18)$$

where $\hat{F}^{\alpha,\alpha',\alpha''}$ or $\hat{I}^{\alpha,\alpha',\alpha''}$ are the matrices of the octupole angular momentum of the particle with spin F or I , λ_o is a coupling of the octupole interaction.

On the bare level (before starting the poor-man's scaling procedure), there is a single coupling constant λ_0 . Therefore, all the four coefficients λ_p , λ_d , λ_q and λ_o are simply related to λ_0 . Straightforward analysis shows that the Hamiltonians (12) and (14) are identical provided,

$$\lambda_p = \frac{\lambda_0}{6}, \quad \lambda_d = \frac{26\lambda_0}{525}, \\ \lambda_q = -\frac{\lambda_0}{840}, \quad \lambda_o = -\frac{\lambda_0}{1890}. \quad (19)$$

It is important that the dimensionless coupling

$$\Lambda_0 = \frac{\lambda_0 \rho_0 k_F}{a_g^2} = \frac{\lambda_0 k_F}{2\hbar\Omega_g a_g^2},$$

has a finite continuous limit $\Omega_g \rightarrow 0$ and $a_g \rightarrow \infty$. Indeed, taking into account eq. (A21) and assuming $\Omega_g \rightarrow 0$ and $a_g \rightarrow \infty$, we can write

$$\frac{1}{2\hbar\Omega_g a_g} = \frac{M}{4\hbar^2}, \quad (20)$$

where M is the atomic mass.

Note that on deriving the exchange Hamiltonian (12), we neglect the spin-orbit and hyperfine interactions. It can be shown that taking into account the spin-orbit and hyperfine interactions modify the Hamiltonian (12), but leave the Hamiltonian (14), [as well as the dipole, quadrupole and octupole interactions (16), (17) and (18)] unchanged, except for slight modifications of the couplings λ_d , λ_q and λ_o . Indeed, as it is shown in Appendix F, the Hamiltonian (14) obeys spin-rotation SU(2) symmetry. The spin-orbit and hyperfine interactions satisfy the same SU(2) symmetry⁴². As a result, the spin-orbit and hyperfine interactions cannot change the Hamiltonian (14).

B. The total Hamiltonian

Having established the explicit expression for the Kondo Hamiltonian, we can now write down the total Hamiltonian of the system by adding the kinetic energy of the itinerant atoms and the atomic energy of the impurity atom. Thus,

$$H = H_0 + H_K, \quad H_0 = H_c + H_{\text{imp}}, \quad (21)$$

where H_c is the Hamiltonian of the itinerant atoms without impurity and H_{imp} is the Hamiltonian of the isolated impurity,

$$H_c = \sum_{n,i} \varepsilon_n c_{n,i}^\dagger c_{n,i}, \quad (22)$$

$$H_{\text{imp}} = \varepsilon_{\text{imp}} \sum_f X^{f,f}. \quad (23)$$

The energy dispersion is [see Appendix A for details]

$$\varepsilon_n = \hbar \Omega_g \left(2n + \frac{3}{2} \right), \quad (24)$$

where Ω_g is the harmonic frequency (A21).

The density of states (DOS) due to the Hamiltonian (22) is

$$\rho(\epsilon) = \frac{1}{2\hbar\Omega_g}, \quad (25)$$

where $\Theta(\xi)$ is the Heaviside theta function equal to 0 for $\xi < 0$, 1 for $\xi > 0$ and $\frac{1}{2}$ for $\xi = 0$.

The Kondo Hamiltonian H_K is given by eq. (14).

V. SECOND ORDER POOR MAN'S SCALING

Section V main points: In this section we derive the poor-man scaling equations to second-order in the exchange constant. This procedure is quite standard, and yet, there are important differences between the procedure applied here and that employed in the standard Kondo effect. First, as we see from Eqs. (28), there are three coupling constants that satisfy a set of three coupled non-linear scaling equations, and second, within the underlying representation of $SU(2)$ the number of spin projections $2s + 1 > 2$.

Applying the poor man's scaling RG procedure to second order enables one to determine the Kondo temperature and, (later on), to derive scaling equations for the exchange coefficients and identifying the fixed points. As far as dipolar interaction is concerned, this procedure is quite standard, but some technical modifications are required for treating multipolar exchange interactions. We start, as usual, by dividing the "conduction" band of (neutral) itinerant atoms defined by $\{\epsilon\}$, such that $|\epsilon - \epsilon_F| < D$ (where ϵ_F is the Fermi energy) into three

parts. The first part contains energies of particle and hole states within a reduced conduction band $|\epsilon - \epsilon_F| < D'$ ($D' = D - \delta D$) which are retained and the second and third parts contains energies of particle and hole states within narrow intervals $D' < |\epsilon - \epsilon_F| < D$ which, within the RG procedure are to be integrated out⁴.

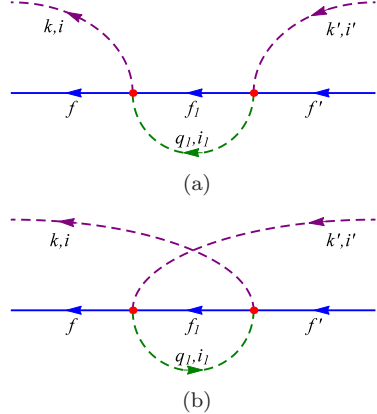


FIG. 3: (color online) "Particle" [panel (a)] and "hole" [panel (b)] second order diagrams for the Kondo Hamiltonian (12). The solid lines correspond to the localized impurity atom, the purple dashed curves describes itinerant atoms before or after the scattering, and the green dashed curves describe itinerant atom in the virtual state near the top edge [panel (a)] or bottom edge [panel (b)] of the conduction band.

Second order corrections to the Kondo Hamiltonian are schematically illustrated in Fig. 3. Here the solid blue line describes the quantum state of the localized impurity. The dashed purple curve restricted from one side by the red dot describes itinerant atom (before or after scattering) whose energy is close to the Fermi energy. The dashed green curves restricted by red dots from both sides describe itinerant atom in the virtual state with the energy within the interval $D' < \epsilon - \epsilon_F < D$ (as in Fig. 3(a)) or $-D < \epsilon - \epsilon_F < -D'$ (as in Fig. 3(b)). The red dots denote the Kondo Hamiltonian (14). Since H_K has three terms, the second order corrections to H_K can be written as,

$$\delta H_2 = \sum_{\beta, \beta'} \delta H_{\beta, \beta'}^{(2)}. \quad (26)$$

Here $\beta, \beta' = d, q, o$ for dipole, quadrupole and octupole interaction,

$$\begin{aligned} \delta H_{\beta, \beta'}^{(2)} = & \frac{1}{2} \sum_{e, e'} H_\beta |e\rangle \langle e| \frac{1}{\epsilon_0 - H_0} |e'\rangle \langle e'| H_{\beta'} + \\ & + \frac{1}{2} \sum_{e, e'} H_{\beta'} |e\rangle \langle e| \frac{1}{\epsilon_0 - H_0} |e'\rangle \langle e'| H_\beta, \end{aligned} \quad (27)$$

where $|e\rangle$ and $|e'\rangle$ are quantum states with a hole near the Fermi energy and an atom with energy in the interval $D' < \epsilon < D$, or a hole on an energy level in the interval $-D < \epsilon < -D'$ and an additional atom near the Fermi level. H_0 is the Hamiltonian of itinerant atoms without

impurity. For $\delta D \ll D$, we can use the approximation,

$$\left\langle e \left| \frac{1}{\epsilon_0 - H_0} \right| e' \right\rangle \approx -\frac{1}{D} \delta_{e,e'}.$$

Explicit expressions for the operators $\delta H_{\beta,\beta'}^{(2)}$ are derived in Appendix C. Combining all the differentials $\delta H_{\beta,\beta'}^{(2)}$, we see that integrating out the virtual states near the band edges to lowest order results in a new Hamiltonian of the *same form* as eq. (14) but with renormalized coupling constants $\lambda_\beta(D) \rightarrow \lambda_\beta(D') = \lambda_\beta(D) + \delta\lambda_\beta$, where $\beta = d, q, o$. Consequently, we arrive at the following second order poor man's scaling equations for the dimensionless couplings $\Lambda_\beta = \lambda_\beta \rho_0$,

$$\frac{\partial \Lambda_d}{\partial \ln D} = -\Lambda_d^2 - \frac{9216}{25} \Lambda_q^2 - \frac{1469664}{25} \Lambda_o^2, \quad (28a)$$

$$\frac{\partial \Lambda_q}{\partial \ln D} = -12\Lambda_d \Lambda_q - \frac{1458}{5} \Lambda_q \Lambda_o, \quad (28b)$$

$$\frac{\partial \Lambda_o}{\partial \ln D} = -18\Lambda_d \Lambda_o - \frac{64}{9} \Lambda_q^2 + \frac{306}{5} \Lambda_o^2. \quad (28c)$$

Here $\rho_0 = \rho(0)$ is the density of states (25) of itinerant atoms at the Fermi energy [which is assumed to be zero here].

The initial values $\Lambda_\beta^{(0)} = \Lambda_\beta(D_0)$ of the couplings Λ_β (where $\beta = d, q, o$) are,

$$\Lambda_d^{(0)} = \frac{26}{525} \frac{\lambda_0 \rho_0 k_F}{a_g^2}, \quad (29a)$$

$$\Lambda_q^{(0)} = -\frac{1}{840} \frac{\lambda_0 \rho_0 k_F}{a_g^2}, \quad (29b)$$

$$\Lambda_o^{(0)} = -\frac{1}{1890} \frac{\lambda_0 \rho_0 k_F}{a_g^2}. \quad (29c)$$

Note that when the initial values of Λ_q and Λ_o are zero, the right hand sides of eqs. (28b) and (28c) vanish and the set of equations (28) reduces to the standard scaling equation for the s-d Kondo model⁴,

$$\frac{\partial \Lambda_d}{\partial \ln D} = -\Lambda_d^2. \quad (30)$$

In the next section we elucidate the effect of the quadrupole and octupole interactions on the scaling invariant of the RG equations, that is, the Kondo temperature⁴ and show that it is rather significant.

It should be noted that the scaling procedure is carried out until the effective bandwidth D essentially exceeds $\hbar\omega_g$ and T_K [where T_K is the Kondo temperature defined below]. In what follows, we assume that $\hbar\omega_g < T_K$, and therefore the Kondo temperature is the infrared cutoff parameter of our theory.

VI. KONDO TEMPERATURE

Section VI main points: Based on the results of the previous section the Kondo temperature is calculated and

estimated numerically. It is shown that this central parameter is within an experimental reach.

The Kondo temperature is defined as the value of D for which the running coupling constants $\Lambda_\beta(D)$ diverge ($\beta = d, q, o$). We solve the set of equations (28) numerically for different initial values $\Lambda_\beta^{(0)}$. Using eq. (29), we can express $\Lambda_q^{(0)}$ and $\Lambda_o^{(0)}$ in terms of $\Lambda_d^{(0)}$. Then the Kondo temperature is a function of a single parameter, $\Lambda_d^{(0)}$. The results of these numerical calculations for the Kondo temperature are displayed in Fig. 4, (solid curve). T_K can be approximated by the following expression,

$$T_K = D_0 \exp \left(-\frac{1}{A \Lambda_d^{(0)}} \right), \quad A = 13.9594. \quad (31)$$

The approximation (31) for T_K is displayed in Fig. 4, (dashed curve). It is clearly seen that the dashed and solid curves are close to each other, so that the approximation (31) is satisfactory.

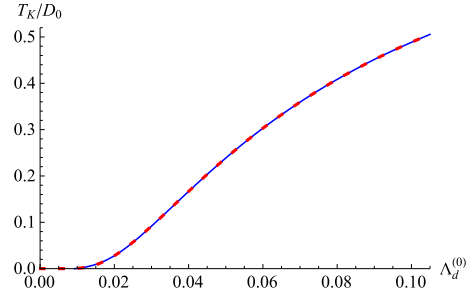


FIG. 4: (color online) Kondo temperature calculated numerically from the set of equations (28) [solid blue curve] and the approximation (31) [dashed red curve].

Note that the scaling equation (30) yields the following expressions for the Kondo temperature,

$$T_K^{(d)} = D_0 \exp \left(-\frac{1}{\Lambda_d^{(0)}} \right). \quad (32)$$

The factor $A \gg 1$ in eq. (31) indicates that the quadrupole and octupole interactions are important and act to enhance T_K . Numerical calculations give $0.03D_0 < T_K < 0.1D_0$ for $400 \text{ nK} < T_F < 1000 \text{ nK}$. When $D_0 = 300 \text{ nK}$, the Kondo temperature is $8 \text{ nK} < T_K < 30 \text{ nK}$, so that the Kondo effect can be measured in experiment.

VII. THIRD ORDER POOR MAN'S SCALING

Section VII main points: A necessary (but not sufficient) condition for arriving at a novel fixed point is to check that such point is a *finite solution of third order scaling equations*. Derivation and solutions of these equations is carried out in this section. As expected, the calculations are rather involved due to the occurrence of higher multiples, third order diagrams and spin $s > \frac{1}{2}$. Nevertheless, these cumbersome calculations should not mask

the important physical consequence that there are three candidates for stable finite fixed points P_4, P_5 and P_7 , that correspond to non-Fermi liquid ground-states.

In order to derive the third order correction to the poor-man's scaling equations (28), we need to consider the second order correction to the energy of the system, as encoded in the self energy diagrams shown in Fig. 5, as well as the third order vertex diagrams shown in Fig. 6 (see Ref.⁴). These diagrams are considered below each one in its turn.

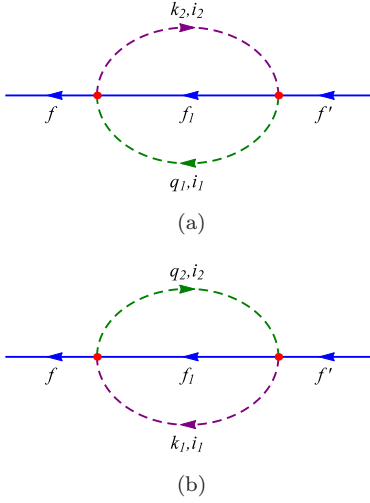


FIG. 5: (color online) “Particle” [panel (a)] and “hole” [panel (b)] second order self energy diagrams. The solid lines correspond to the localized impurity atom, the purple dashed curves restricted by the vertex from one side describe itinerant atoms before or after the scattering, the purple dashed curves restricted by vertex from both sides describe itinerant atoms in the virtual state in the reduced energy band and the green dashed curves describe itinerant atom in the virtual state near the top edge [panel (a)] or bottom edge [panel (b)] of the conduction band.

A. Second Order Self Energy Diagrams

Second order correction to the energy is illustrated by diagrams in Fig. 5.

The second order corrections to the self energy are calculated in Appendix D. Taking into account eqs. (D5), (D8) and (D10), we get

$$\delta E = -\frac{\delta D}{D} E \left\{ \frac{525}{4} \Lambda_d^2 + 13440 \Lambda_q^2 + 3306744 \Lambda_o^2 \right\}. \quad (33)$$

B. Third Order Vertex Diagrams

Now we consider in details the third order contributions to the scaling equations given by diagrams in Fig.

6. The corresponding correction to the Kondo Hamiltonian is decomposed as,

$$\delta H_3 = \sum_{\beta, \beta'} \delta H_{\beta', \beta, \beta'}^{(3)}, \quad (34)$$

where $\beta, \beta' = d, q, o$ for the dipole, quadrupole and octupole interactions,

$$\begin{aligned} \delta H_{\beta', \beta, \beta'}^{(3)} = & \frac{\lambda_\beta \lambda_{\beta'}^2}{D^2} \frac{k_F^3}{a_g^6} \times \\ & \times \sum_{\vec{\alpha}_\beta, \vec{\alpha}'_{\beta'}} \sum_{f, f'} \left(\hat{F}^{\vec{\alpha}_\beta} \hat{F}^{\vec{\alpha}_\beta} \hat{F}^{\vec{\alpha}'_{\beta'}} \right)_{f, f'} \times \\ & \times X^{f, f'} \sum_{i, i'} \sum_{n, n'} I_{i, i'}^{\vec{\alpha}_\beta} c_{n, i}^\dagger c_{n', i'} \times \\ & \times \text{Tr} \left(\hat{I}^{\vec{\alpha}_\beta} \hat{I}^{\vec{\alpha}'_{\beta'}} \right) \mathfrak{G}. \end{aligned} \quad (35)$$

Here $\hat{F}^{\vec{\alpha}_\beta}$ or $\hat{I}^{\vec{\alpha}_\beta}$ are dipole ($\beta = d$), quadrupole ($\beta = q$) and octupole ($\beta = o$) matrices for a localized impurity or itinerant atoms, $\vec{\alpha}_d \equiv \alpha$, $\vec{\alpha}_q \equiv (\alpha, \alpha')$ and $\vec{\alpha}_o \equiv (\alpha, \alpha', \alpha'')$, where α 's are Cartesian indices [see eqs. (2), (3) and (5)]. The quantity \mathfrak{G} is

$$\mathfrak{G} = 2\rho_0^2 D \delta D. \quad (36)$$

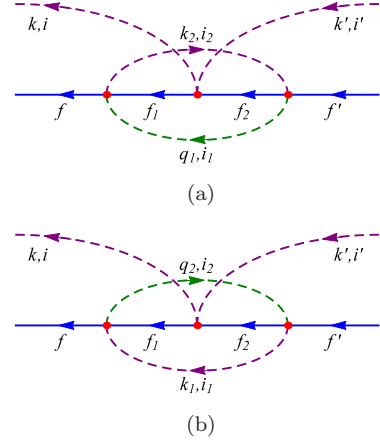


FIG. 6: (color online) “Particle” [panel (a)] and “hole” [panel (b)] third order diagrams for the Kondo Hamiltonian (12). The solid lines correspond to the localized impurity atom, the purple dashed curves restricted by the vertex from one side describe itinerant atoms before or after the scattering, the purple dashed curves restricted by vertex from both sides describe itinerant atoms in the virtual state in the reduced energy band and the green dashed curves describe itinerant atom in the virtual state near the top edge [panel (a)] or bottom edge [panel (b)] of the conduction band.

Explicit expressions for the operators $\delta H_{\beta', \beta, \beta'}^{(3)}$ are derived in Appendix E. It is shown there that $H_K + \delta H_2 + \delta H_3$ has the *same form* as H_K , albeit with proper corrections to the coupling constants $\lambda_\beta + \delta \lambda_\beta$. Therefore we conclude that inclusion of δH_3 does not change the structure of the initial Kondo Hamiltonian, but it gives rise to an additional renormalization of the couplings λ_β .

C. Third Order Poor Man's Scaling Equations

The effective Hamiltonian (which includes energy and vertex renormalization) depends on the energy E^4 which is determined through the Schrödinger equation

$$H\Psi = E\Psi,$$

and this dependence is given by⁴

$$\tilde{H}_{\text{eff}}(E) = \tilde{H}_{\text{eff}}(0) - ES,$$

where the parameter $S = \delta E/E$ does not depend on E , see eq. (33), and

$$\tilde{H}_{\text{eff}}(0) = H_K + \delta H_2 + \delta H_3, \quad (37)$$

δH_2 and δH_3 are given by eqs. (26) and (34). In order to get an effective Hamiltonian, we solve the (implicit) secular equation,

$$|\tilde{H}_{\text{eff}}(E) - E| = 0,$$

(where $|A|$ denotes the determinant of the square matrix A) which leads to

$$|\tilde{H}_{\text{eff}}(0) - (1 + S)E| = 0.$$

This equation gives an E -independent Hamiltonian,

$$H_{\text{eff}} = (1 + S)^{-1/2} \tilde{H}_{\text{eff}}(0) (1 + S)^{-1/2}.$$

Taking into account that $S \sim \lambda^2$ [see eq. (33)] and keeping the terms up to λ^3 , we can write H_{eff} as,

$$H_{\text{eff}} = H_K + \delta H_2 + \delta \tilde{H}_3, \quad (38)$$

where

$$\delta \tilde{H}_3 = \delta H_3 + S H_K. \quad (39)$$

Taking into account the results of subsections VII A and VII B, we can see that the operator $\delta \tilde{H}_3$ has the same form as the Hamiltonian H_K , (see eq. (14) and the equations below it). Therefore, it gives rise to renormalization of the couplings constants λ_β . The third order poor-man scaling equations for the dimensionless couplings $\Lambda_\beta = \lambda_\beta \rho_0$ are,

$$\frac{\partial \Lambda_\beta}{\partial \ln D} = \mathfrak{F}_\beta(\Lambda_d, \Lambda_q, \Lambda_o), \quad (40)$$

where $\beta = d, q, o$, the functions $\mathfrak{F}_{d,q,o}$ are,

$$\begin{aligned} \mathfrak{F}_d &= -\Lambda_d^2 - \frac{9216}{25} \Lambda_q^2 - \frac{1469664}{25} \Lambda_o^2 + 35 \Lambda_d^3 + \\ &+ 12096 \Lambda_d \Lambda_q^2 + \frac{21493836}{5} \Lambda_d \Lambda_o^2, \end{aligned} \quad (41a)$$

$$\begin{aligned} \mathfrak{F}_q &= -12 \Lambda_d \Lambda_q - \frac{1458}{5} \Lambda_q \Lambda_o + \frac{945}{8} \Lambda_q \Lambda_d^2 + \\ &+ 17472 \Lambda_q^3 + \frac{15380348}{5} \Lambda_q \Lambda_o^2, \end{aligned} \quad (41b)$$

$$\begin{aligned} \mathfrak{F}_o &= -18 \Lambda_d \Lambda_o - \frac{64}{9} \Lambda_q^2 + \frac{306}{5} \Lambda_o^2 + \frac{1365}{8} \Lambda_o \Lambda_d^2 + \\ &+ 12096 \Lambda_o \Lambda_q^2 + \frac{16769916}{5} \Lambda_o^3. \end{aligned} \quad (41c)$$

The symmetry of the scaling equations (40) should be noted: \mathfrak{F}_d and \mathfrak{F}_o are even with respect to the inversion transformation $\Lambda_q \rightarrow -\Lambda_q$, whereas \mathfrak{F}_q is odd. Therefore we can safely conclude that the scaling equations (40) are invariant with respect to the inversion $\Lambda_q \rightarrow -\Lambda_q$. The fixed points of the scaling equations (40) are found from the conditions, $\mathfrak{F}_{d,q,o} = 0$. Numerical solution of the last set of equations yields seven fixed points in 3D parameter space, $P_n = (\Lambda_d^{(n)}, \Lambda_q^{(n)}, \Lambda_o^{(n)})$, $n = 1, 2, \dots, 7$:

$$P_1 = (0.0285714, 0, 0), \quad (42a)$$

$$P_2 = (0.0193713, -0.00192056, -0.000158648), \quad (42b)$$

$$P_3 = (0.0193713, 0.00192056, -0.000158648), \quad (42c)$$

$$P_4 = (0.0147126, -0.00101842, 0.00026056), \quad (42d)$$

$$P_5 = (0.0140075, 0, -0.000264616), \quad (42e)$$

$$P_6 = (0.0140587, 0, 0.000246764), \quad (42f)$$

$$P_7 = (0.0147126, 0.00101842, 0.00026056). \quad (42g)$$

There is one more fixed point, $P_0 = (0, 0, 0)$, but it is unstable, see scaling equations (28).

The scaling pattern of the parameters Λ_β ($\beta = d, q, o$) depends on the initial values of the parameters. The initial values of Λ_β are given by eq. (29) [see also eq. (19)]. They consist of the dimensionless parameter $\lambda_0 \rho_0$ which is calculated from a microscopic model of interaction of a Yb atom in the 1S_0 state with an Yb atom in the 3P_2 state, see eq. (8). It is seen that Λ_d is positive, whereas Λ_q and Λ_o are negative.

To proceed further, it is necessary to study the scaling of Λ_d , Λ_q and Λ_o near the fixed points $P_n = (\Lambda_d^{(n)}, \Lambda_q^{(n)}, \Lambda_o^{(n)})$. For this purpose we introduce the variables x_d , x_q and x_o ,

$$\begin{aligned} \Lambda_d &= \Lambda_d^{(n)} + x_d, \\ \Lambda_q &= \Lambda_q^{(n)} + x_q, \\ \Lambda_o &= \Lambda_o^{(n)} + x_o, \end{aligned}$$

and assume that x_β [$\beta = d, q, o$] are small. Expanding the functions \mathfrak{F}_β , eq. (41), in x_β to first (linear) order we get,

$$\mathfrak{F}_\beta(\Lambda_d, \Lambda_q, \Lambda_o) = \sum_{\beta' = d, q, o} A_{\beta, \beta'} x_{\beta'} + O(x^2),$$

where

$$A_{\beta, \beta'} = \left(\frac{\partial \mathfrak{F}_\beta}{\partial \Lambda_{\beta'}} \right)_{P_n},$$

the derivative is taken at the fixed point P_n . Thereby we get a set of linear differential equations for x_β ,

$$\frac{\partial x_d}{\partial \ln D} = A_{d,d} x_d + A_{d,q} x_q + A_{d,o} x_o, \quad (43a)$$

$$\frac{\partial x_q}{\partial \ln D} = A_{q,d} x_d + A_{q,q} x_q + A_{q,o} x_o, \quad (43b)$$

$$\frac{\partial x_o}{\partial \ln D} = A_{o,d} x_d + A_{o,q} x_q + A_{o,o} x_o. \quad (43c)$$

The solution of the set of equations (43) is of the form,

$$x_\beta \propto D^\gamma,$$

where the Lyapunov exponent γ is an eigenvalue of the set of equations (43). The set of three linear equations has, as a rule, three eigenvalues. A fixed point P_n is stable when all x_β tend to zero as D tends to zero. This occurs when all γ 's are positive. Accordingly, we now write down the numerical values of the triples $(\gamma_1, \gamma_2, \gamma_3)$ for each one of the fixed points $P_1 - P_7$ in its turn and determine its stability (s=stable, u=unstable).

$$\begin{aligned} P_1 : (\gamma_1, \gamma_2, \gamma_3) &= (0.0285714, -0.246429, -0.375) \Rightarrow u. \\ P_2 : (\gamma_1, \gamma_2, \gamma_3) &= (0.341287, -0.228946, 0.163813) \Rightarrow u. \\ P_3 : (\gamma_1, \gamma_2, \gamma_3) &= (0.341287, -0.228946, 0.163813) \Rightarrow u. \\ P_4 : (\gamma_1, \gamma_2, \gamma_3) &= (0.44974, 0.320668, 0.0632014) \Rightarrow s. \\ P_5 : (\gamma_1, \gamma_2, \gamma_3) &= (0.434777, 0.14764, 0.14764) \Rightarrow s. \\ P_6 : (\gamma_1, \gamma_2, \gamma_3) &= (0.40609, 0.271873, -0.0300051) \Rightarrow u. \\ P_7 : (\gamma_1, \gamma_2, \gamma_3) &= (0.44974, 0.320668, 0.0632014) \Rightarrow s. \end{aligned}$$

Note that P_1 is the NB fixed point, that in this case is unstable. Accordingly, only P_4 , P_5 and P_7 are stable. Elucidation of these three stable fixed points such that the corresponding fixed point Hamiltonians display non-Fermi liquid behavior (see section IX) is one of the central results of the present work.

VIII. ANALYSIS OF THE SCALING EQUATIONS

Section VIII main points: Analysis of the flow pattern for a system of three coupled non-linear scaling equations is rather rich and complicated. To some extent, in Figs. 7 and 8, we work out the analogue of the celebrated Anderson-Yuval equations (derived for the anisotropic KE), as adapted for the present model. Unlike the former case, however, where the fixed points are at infinity, the present analysis leads to the occurrence of finite fixed points.

Let us consider the scaling equations (40) in some details. Note that when $\Lambda_q = \Lambda_o = 0$, then we recover the s-d model as a special case. In this case, scaling of Λ_d depends on the sign of $\Lambda_d^{(0)}$. For $\Lambda_d^{(0)} > 0$ $\Lambda_d(D)$ flows towards the Nosièr-Blandin fixed point P_1 , eq. (42a) indicating an over-screened KE. When $\Lambda_d^{(0)} < 0$, $\Lambda_d(D)$ flows towards zero which means that there is no KE. When $\Lambda_q^{(0)}$ and/or $\Lambda_o^{(0)}$ are nontrivial, the scenario is more complicated. In order to analyze scaling, we consider the following equations,

$$\frac{\partial \Lambda_q}{\partial \Lambda_d} = \frac{\mathfrak{F}_q(\Lambda_d, \Lambda_q, \Lambda_o)}{\mathfrak{F}_d(\Lambda_d, \Lambda_q, \Lambda_o)}, \quad (44a)$$

$$\frac{\partial \Lambda_o}{\partial \Lambda_d} = \frac{\mathfrak{F}_o(\Lambda_d, \Lambda_q, \Lambda_o)}{\mathfrak{F}_d(\Lambda_d, \Lambda_q, \Lambda_o)}, \quad (44b)$$

where $\mathfrak{F}_{d,q,o}$ are given by eq. (41). Solving the set of equations (44), we get Λ_q and Λ_o as functions of Λ_d .

Numerical solution of the set of equations is illustrated in Figs. 7 and 8. It is seen that there are the following scaling regimes:

- All the couplings Λ_β flow to zero when D vanishes. In this case there is no KE.
- The couplings Λ_β flow to one of the stable fixed points. In this case, there is KE.

First, we should determine for which values of the couplings $\Lambda_\beta^{(0)}$ there is KE, and for which ones there is no KE. Our numerical analysis shows that when $\Lambda_d > 0$, there is *always* KE (see Fig. 8). Therefore we investigate the case $\Lambda_d^{(0)} < 0$. The result of our numerical calculations for this case is shown in Fig. 7. Let us analyze the different scaling regimes displayed in this figure.

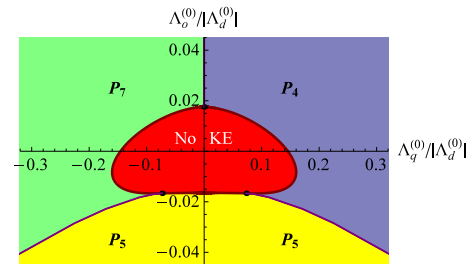


FIG. 7: (color online) Scaling of Λ_d , Λ_q and Λ_o for $\Lambda_d^{(0)} = -0.00105$ and different values of $\Lambda_q^{(0)}$ and $\Lambda_o^{(0)}$. The red area: all Λ 's flow to zero and there is no KE. Yellow area: Λ 's flow to the fixed point P_5 . Blue area: Λ 's flow to the fixed point P_4 . Green area: Λ 's flow to the fixed point P_7 .

When the effective bandwidth decreases, the coupling Λ_d increases from its negative initial value and tends to 0. At this stage, it is important to determine whether $|\Lambda_q(D)|$ and $|\Lambda_o(D)|$ decrease faster or slower than $|\Lambda_d(D)|$. In other words, we should consider the dimensionless parameters \mathcal{K}_β ($\beta = d, q, o$), defined as,

$$\mathcal{K}_\beta = \frac{\partial \ln |\Lambda_\beta(D_0)|}{\partial \ln D_0}.$$

(For $\Lambda_d < 0$, all \mathcal{K}_β are positive). When $\mathcal{K}_d < \mathcal{K}_{q,o}$, the couplings $\Lambda_{q,o}$ vanish faster than Λ_d . As a result, the Kondo Hamiltonian renormalizes towards the s-d model Hamiltonian with ferromagnetic coupling $\Lambda_d(D)$. This coupling flows towards zero when D vanishes. This is the case when Λ_β are in the red area in Fig. 7 (see also dark red arrowed curves in Fig. 8).

When $\mathcal{K}_q < \mathcal{K}_d$ and/or $\mathcal{K}_o < \mathcal{K}_d$, then Λ_d vanishes when Λ_q and/or Λ_o assume finite values. At this point, Λ_β continues to flow [see eqs. (40) and (41)]. Λ_d , for example, changes its sign and the couplings Λ_β flow towards one of the fixed points, P_4 , P_5 or P_7 (blue, yellow and green areas in Fig. 7). Note that quadrupole and octupole interaction give rise to exotic property of the KE: *The effective dipole coupling $\Lambda_d(T)$ as a function of temperature turns from ferromagnetic at high temperature to antiferromagnetic at low temperature*. This property is shown in Fig. 8, see orange and green arrowed curves.

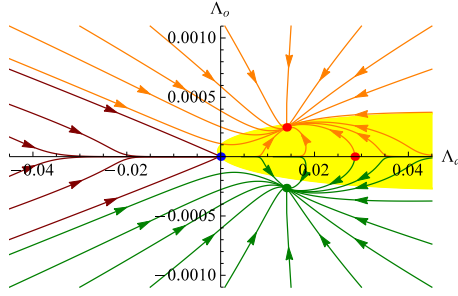


FIG. 8: (color online) Scaling of Λ_d and Λ_o for $\Lambda_q = 0$. Dark red arrowed lines: the couplings rescale to zero. Green lines: the couplings renormalize towards the stable fixed point P_5 , eq. (42e). Orange lines: the couplings renormalize towards the saddle fixed point P_6 , eq. (42f). When Λ_q is very small but not zero, the couplings renormalize towards the fixed points P_4 or P_7 , eqs. (42d) or (42g) depending either the initial value of Λ_q is negative or positive.

It should be noted that when $\Lambda_q = 0$, the function $\mathfrak{F}_q = 0$ [see eq. (41b)]. Therefore, when $\Lambda_q^{(0)} = 0$, then $\Lambda_q(D) = 0$ for any $D < D_0$. Consider renormalization of Λ_d and Λ_o in the plane $\Lambda_q = 0$. Numerical solution of eq. (44b) for $\Lambda_q(0) = 0$ is displayed in Fig. 8. It is seen that the couplings flow to one of the fixed points, P_0 , P_5 or P_6 , eq. (42). In order to check stability of the solution, we apply the Lyapunov method for stability. For this purpose, we consider the scaling equation for $\Lambda_q(D)$,

$$\frac{\partial \Lambda_q}{\partial \ln D} = \mathfrak{F}_q(\Lambda_d, \Lambda_q, \Lambda_o),$$

with infinitesimal initial condition $\Lambda_q^{(0)}$. Keeping just the linear power of Λ_q on the right hand side of the last equation we may write,

$$\frac{\partial \Lambda_q}{\partial \ln D} = \Lambda_q \mathcal{A}_q(\Lambda_d, \Lambda_o), \quad (45)$$

where

$$\mathcal{A}_q(\Lambda_d, \Lambda_o) = \lim_{\Lambda_q \rightarrow 0} \left(\frac{\partial \mathfrak{F}_q(\Lambda_d, \Lambda_q, \Lambda_o)}{\partial \Lambda_q} \right).$$

The solution of eq. (45) is,

$$\frac{\Lambda_q(D)}{\Lambda_q^{(0)}} = \exp \left\{ - \int_D^{D_0} \mathcal{A}_q(\Lambda_d(D'), \Lambda_o(D')) \frac{dD'}{D'} \right\}. \quad (46)$$

Note that when D vanishes, Λ_d and Λ_o flow to one of the fixed points (42), where \mathcal{A}_q takes a finite value. In this case the integral on the right hand side of eq. (46) diverges. Thus, we conclude that when \mathcal{A}_q is positive along all the scaling trajectories of $\Lambda_d(D)$ and $\Lambda_o(D)$, then $\Lambda_q(D)$ flows to zero, and the solution displayed in Fig. 8 is stable. When \mathcal{A}_q is negative, then $\Lambda_q(D)$ flows away from zero, and the solution displayed in Fig. 8 is unstable. The interval of Λ_d and Λ_o where the solution displayed in Fig. 8 is unstable is marked by yellow.

Finally, we just state our result pertaining to scaling of the couplings satisfying the initial conditions (29). Numerical analysis shows that for any positive λ_0 , the couplings flow towards the fixed point P_5 .

IX. STRONG COUPLING REGIME

Section IX main points: Before studying experimental issues it is useful to elucidate the nature of the ground state. This will determine whether the pertinent Kondo physics at the stable points is that of over-screening or under screening. Thus, after the candidates for stable fixed points are identified, it is necessary to elucidate the ground-state wave functions at these points. The reason is at least two-fold. First, it is required in order to evaluate physical observables. Second, it is essential to determine whether the strong coupling fixed point is unstable, so that according to NB analysis, there is a stable finite fixed point, and over-screening does occur. This task is carried out below, using variational wave functions. It is then found that the nature of the system (whether there is or there is no over-screening) depends on the initial value of the bare constants λ_d , λ_q and λ_o . Similar (albeit simpler) situation is encountered in the two-channel KE based on the $s - d$ Hamiltonian.

The variational method is an appropriate tool for that purpose, which is not based on perturbation theory. It can be shown that the minimal energy can be reached when the number of atoms over the fully occupied Fermi sphere is $\mathcal{N} = I + \frac{1}{2}$. For $I = \frac{5}{2}$, $\mathcal{N} = 3$. Such a three particle wave function is described by the three atomic spin S . The maximal value of the spin is $S = \frac{9}{2}$. This value can be get as following: according to the Pauli principle, the magnetic quantum numbers satisfy the inequalities $i_1 \neq i_2$, $i_2 \neq i_3$ and $i_3 \neq i_1$. Therefore the maximal magnetic quantum number of the three atoms is $S = \frac{9}{2}$.

A simple form of variational wave function is,

$$|L, m\rangle = \sum_{f, \{i\}_3, \{n\}_3} C_{S, s; F, f}^{L, m} \psi_L(n_1) \psi_L(n_2) \psi_L(n_3) \times C_{I, i_1; I, i_2; I, i_3}^{S, s} c_{n_1, i_1}^\dagger c_{n_2, i_2}^\dagger c_{n_3, i_3}^\dagger |f; \Omega\rangle, \quad (47)$$

where $|f; \Omega\rangle$ describes the impurity with magnetic quantum number f and a Fermi sea with all the levels below the Fermi energy occupied and all the levels above the Fermi energy free. $C_{S, s; F, f}^{L, m}$ are the appropriate Clebsch-Gordan coefficients, and $L = S + F, S + F - 1, S + F - 2, \dots, S - F$ is the total angular momentum of the four atomic system. $C_{I, i_1; I, i_2; I, i_3}^{S, s}$ are so called three particle Clebsch-Gordan coefficients. Here we use the fact that H_d , H_q and H_o commute with each other (see Appendix F for details), and therefore the four-atomic orbital angular momentum L is a good quantum number.

In order to find $\psi_L(n)$, we apply the Schrödinger equation

$$H|L, m\rangle = \varepsilon|L, m\rangle.$$

Then we get

$$(\varepsilon_n - \varepsilon)\psi_L(n) + g_L \sum_{n'} \Theta(\varepsilon_{n'} - \varepsilon_F)\psi_L(n') = 0. \quad (48)$$

Here

$$g_L = \left\{ \lambda_d \mathcal{D}_L + \lambda_q \mathcal{Q}_L + \lambda_o \mathcal{O}_L \right\} \frac{k_F}{a_g^2}, \quad (49)$$

where

$$\begin{aligned} \mathcal{D}_L &= \frac{1}{2} \left\{ L(L+1) - F(F+1) - I(I+1) \right\}, \\ \mathcal{Q}_L &= 4 \mathcal{D}_L^2 + 2 \mathcal{D}_L - \frac{4}{3} F(F+1) S(S+1), \\ \mathcal{O}_L &= 36 \mathcal{D}_L^3 + 72 \mathcal{D}_L^2 + 12 \mathcal{D}_L - \\ &\quad - \frac{12}{5} (3S(S+1) - 1) (2F(F+1) - 1) \mathcal{D}_L - \\ &\quad - 18 S(S+1) F(F+1). \end{aligned}$$

The solution of eq. (48) is,

$$\psi_L(n) = \frac{A_L}{\varepsilon_L - \varepsilon_n},$$

where A_L is a normalization constant. The energy ε_L can be found from the equation,

$$g_L \sum_n \frac{\Theta(\varepsilon_n - \varepsilon_F)}{\varepsilon_L - \varepsilon_n} + 1 = 0. \quad (50)$$

We are interested in the energies ε_L which are below the Fermi energy ε_F . This is the case when $g_L < 0$. Introducing the density of states, we can write,

$$\varepsilon_L - \varepsilon_F = D_0 \exp \left(- \frac{1}{|g_L| \rho_0} \right).$$

The energy of the ground state is found as

$$\varepsilon_{\text{gs}} = \min_L \varepsilon_L.$$

Thus, the problem of finding the ground state reduces to that of finding a minimum of g_L . In order to check whether the magnetic impurity is over-screened or under-screened, we consider the operator

$$(\mathbf{L} \cdot \mathbf{F}) = \frac{1}{2} \{ L(L+1) + F(F+1) - S(S+1) \}. \quad (51)$$

When $(\mathbf{L} \cdot \mathbf{F}) < 0$, there is over-screened KE. Using eq. (51), we get the condition of over-screened KE,

$$L(L+1) + F(F+1) - S(S+1) < 0. \quad (52)$$

When $S = \frac{9}{2}$ and $F = \frac{3}{2}$, the condition (52) is fulfilled when $L = 3$ or 4 . Note that the condition (52) is sufficient but not necessary for over-screened KE: When the condition (52) is fulfilled, there is over-screened KE with non Fermi liquid ground state. When the condition (52)

is not fulfilled, we cannot say about the nature of the ground state.

We now apply our analysis for elucidating the nature of the stable fixed points P_4 , P_5 and P_7 . For the fixed point P_4 , the ground state corresponds to the energy level with $L = 3$, and therefore there is an over-screened KE. Similarly, for the fixed point P_5 , the ground state corresponds to the energy level with $L = 4$, and therefore there is over-screened KE. Finally, for the fixed point P_7 , the ground state corresponds to the energy level with $L = 5$, and therefore we cannot conclude whether the impurity is over-screened or under-screened. As an example, when the initial values of the couplings λ_d , λ_q and λ_o are given by eq. (29), the Kondo Hamiltonian flows toward the fixed point P_5 , and therefore we can conclude that there is an over-screened KE. In order to demonstrate this, let us investigate exchange interaction between the “dressed” impurity atom and the Fermi sea. For this purpose, we assume that the temperature is so low that the “dressed” impurity is in its ground state described by wave functions (47), and apply the following representation of the identity operator,

$$\begin{aligned} &\sum_{n,i,m} c_{n,i}^\dagger |L, m; g\rangle \langle L, m; g| c_{n,i} + \\ &+ \sum_{n,i,m} c_{n,i} |L, m; g\rangle \langle L, m; g| c_{n,i}^\dagger = 1, \end{aligned}$$

where $|L, m; g\rangle$ describes the degenerate Fermi sea of the itinerant atoms and the “dressed” impurity. Then the exchange interaction of the “dressed” impurity with the itinerant atoms is

$$\begin{aligned} \tilde{H}_K &= \sum_{n,n'} \sum_{i,i'} \sum_{m,m'} \left\{ \langle L, m; g | c_{n',i'}^\dagger H_K c_{n,i}^\dagger | L, m'; g \rangle - \right. \\ &\quad \left. - \langle L, m; g | c_{n,i}^\dagger H_K c_{n',i'} | L, m'; g \rangle \right\} Y^{m,m'} c_{n',i'}^\dagger c_{n,i}, \end{aligned}$$

where $Y^{m,m'} = |L, m\rangle \langle L, m'|$. Taking into account eqs. (12) and (47), we can write

$$\begin{aligned} \tilde{H}_K &= \frac{\tilde{\lambda}}{a_g^2} \sum_{n,n'} \sum_{i,i'} \sum_{m,m'} \sum_j \sum_{\{i\}_3} \sum_{\{i'\}_3} Y^{m,m'} c_{n',i'}^\dagger c_{n,i} \times \\ &\quad \times C_{I,i_1;I,i_2;I,i_3;I,i;J,j}^{L,m} C_{I,i'_1;I,i'_2;I,i'_3;I,i';J,j}^{L,m'}, \quad (53) \end{aligned}$$

where $C_{I,i_1;I,i_2;I,i_3;I,i;J,j}^{L,m}$ are the Clebsch-Gordan coefficients, $\{i\}_3 = \{i_1, i_2, i_3\}$ and $\{i'\}_3 = \{i'_1, i'_2, i'_3\}$. The coupling $\tilde{\lambda} \sim T_K$ is positive.

The Hamiltonian (53) can be written as a sum of multiple interactions, similar to the Hamiltonian (14), but because of high spins [the dressed impurity has the spin $L = 4$ and the itinerant atoms have spin $I = \frac{5}{2}$], the exchange Hamiltonian consists of dipole, quadrupole, octupole, 16-pole and 32-pole interactions. Derivation of the scaling equations for this Hamiltonian is much more cumbersome than the derivation of the scaling equations for the bare Hamiltonian (14). Therefore we restrict ourselves by the qualitative analysis of the Hamiltonian (53).

First of all, $\tilde{\lambda} > 0$, and therefore \tilde{H}_K describes an anti-ferromagnetic interaction. This is typical situation for the over-screening KE, where the exchange interaction between the dressed impurity and the Fermi sea is anti-ferromagnetic^{4,8}. It can be shown that in the framework of second order poor man's scaling technique, the anti-ferromagnetic coupling flows towards $\tilde{\lambda} \rightarrow \infty$, and therefore the weak coupling fixed point $\lambda_0 \rightarrow \infty$ is unstable. Taking into account that the $\lambda_0 = 0$ and $\lambda_0 \rightarrow \infty$ weak coupling fixed points are unstable, we can conclude that there is at least one stable strong coupling fixed point with finite λ 's which describes a non Fermi phase⁸.

X. ENTROPY, SPECIFIC HEAT AND MAGNETIC SUSCEPTIBILITY

Section X main points: An appropriate candidate (smoking gun) for an experimental test of the KE in the pertinent system is provided through the temperature dependence of numerous thermodynamic quantities. Here we present results for the impurity contribution to the specific heat, entropy, and the magnetic susceptibility, and compare the first two quantities with those obtained within the standard KE based on the $s-d$ Hamiltonian.

The formalism developed so far enables us to calculate these thermodynamic quantities in the weak coupling regime $T > T_K$, wherein it is expected that the general form of the thermodynamic quantities is dominated by logarithmic functions of $\frac{D}{T}$. Whereas for dipolar exchange interaction (governed by the $s-d$ Hamiltonian), the derivation is quite standard, the derivation and handling of the spin algebra in the present case of multipolar exchange interactions is much more involved. It is found that for the magnetic susceptibility, the temperature dependencies in the standard and multipolar Kondo effect are quite close to each other but for the specific heat and entropy the differences are quite sizable. We are tempted to expect that in the strong coupling regime, the dependencies will be qualitatively and quantitatively distinct.

A. Entropy and the Specific Heat

Entropy S_{imp} and specific heat C_{imp} of the impurity are

$$S_{\text{imp}} = -k_B \frac{\partial(T \ln Z_{\text{imp}})}{\partial T}, \quad (54)$$

$$C_{\text{imp}} = T \frac{\partial S_{\text{imp}}}{\partial T}. \quad (55)$$

Here Z_{imp} is the partition function of the impurity⁴,

$$Z_{\text{imp}} = \frac{Z}{Z_c}, \quad (56)$$

where Z is the partition function of the total system and Z_c is the partition function of the itinerant atoms without

impurity,

$$Z = \text{Tr}(e^{-\beta H}), \quad Z_c = \text{Tr}(e^{-\beta H_c}).$$

Perturbation calculations give forth order logarithmic terms to the entropy (54),

$$S_{\text{imp}} = k_B \left\{ \ln(2F+1) + Z_3 + Z_4 \ln(\beta D) \right\}, \quad (57)$$

where

$$\begin{aligned} Z_3 = & -\frac{2\pi^2}{3} \left\{ \frac{525}{2} \Lambda_d^3 - \frac{18213545952}{5} \Lambda_o^3 + \right. \\ & + 80640 \Lambda_q^2 \Lambda_d + \\ & \left. + 23514624 \Lambda_q^2 \Lambda_o + 39680928 \Lambda_o^2 \Lambda_d \right\}, \end{aligned} \quad (58)$$

$$\begin{aligned} Z_4 = & -\pi^2 \left\{ 525 \Lambda_d^4 + \frac{656474112}{5} \Lambda_q^4 + \right. \\ & + \frac{50025111034752}{25} \Lambda_o^4 + 1537536 \Lambda_d^2 \Lambda_q^2 + \\ & + 1009659168 \Lambda_d^2 \Lambda_o^2 + 1065996288 \Lambda_d \Lambda_q^2 \Lambda_o - \\ & - \frac{671877472896}{5} \Lambda_d \Lambda_o^3 - \\ & \left. - \frac{767799502848}{25} \Lambda_q^2 \Lambda_o^2 \right\}. \end{aligned} \quad (59)$$

The condition imposing the invariance of the entropy under the poor mans scaling transformation is⁴

$$\begin{aligned} \frac{\partial}{\partial \ln D} \left\{ Z_{\text{imp}}^{(3)}(\Lambda_d, \Lambda_q, \Lambda_o) + \right. \\ \left. + Z_4(\Lambda_d, \Lambda_q, \Lambda_o) \ln \left(\frac{D}{k_B T} \right) \right\} = 0. \end{aligned} \quad (60)$$

Within the accuracy of this equation, when differentiating the second term, we should neglect any implicit dependence on D through the couplings $\Lambda_{d,q,o}$. The renormalization procedure should proceed until the bandwidth D is reduced to the temperature T . At this point, the fourth order of the perturbation theory vanishes and the entropy takes the form,

$$\begin{aligned} S_{\text{imp}} = k_B \left\{ \ln(2F+1) + \right. \\ \left. + Z_3(\Lambda_d(T), \Lambda_q(T), \Lambda_o(T)) \right\}, \end{aligned} \quad (61)$$

where Z_3 (as a function of Λ_d , Λ_q and Λ_o) is given by eq. (58), whereas $\Lambda_{d,q,o}(T)$ are solution of the scaling equations (28).

We now are ready to calculate the specific heat (55),

$$C_{\text{imp}} = k_B \frac{\partial}{\partial \ln T} \left[Z_3(\Lambda_d(T), \Lambda_q(T), \Lambda_o(T)) \right].$$

Taking into account the scaling equation (60), we get

$$C_{\text{imp}} = -k_B Z_4(\Lambda_d(T), \Lambda_q(T), \Lambda_o(T)), \quad (62)$$

where Z_4 (as a function of Λ_d , Λ_q and Λ_o) is given by eq. (59), whereas $\Lambda_{d,q,o}(T)$ are solution of the scaling equations (28).

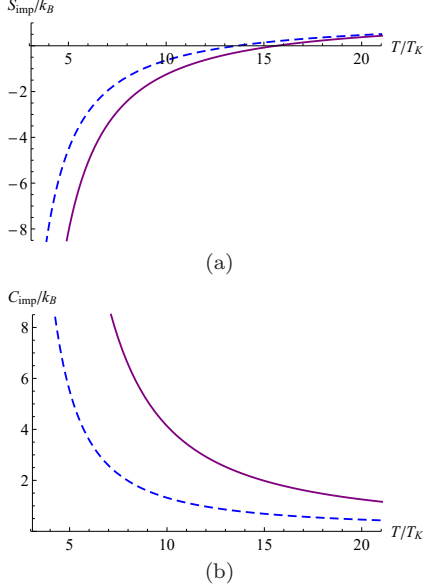


FIG. 9: (color online) Solid curves: The entropy (61) [panel (a)] and the specific heat (62) [panel (b)] for the $^{173}\text{Yb}(^1\text{S}_0) - ^{173}\text{Yb}(^3\text{P}_2)$ system for $\lambda_0 \rho_0 = 0.5$. Dashed curves: The entropy (63) [panel (a)] and the specific heat (64) [panel (b)] for the $^{171}\text{Yb}(^1\text{S}_0) - ^{171}\text{Yb}(^3\text{P}_2)$ system.

The entropy (61) and the specific heat (62) of the impurity are shown in Fig. 9 for $\lambda_0 \rho_0 = 0.5$ [solid curves in panels (a) and (b)]. Fig. 9(a) illustrates decreasing of the entropy due to the Kondo interaction. The entropy of the isolated impurity atom is $\ln(2F + 1)$. Fig. 9(b) demonstrates a Kondo peak in the specific heat.

For comparison with the standard Kondo effect, consider the system consisting of $^{171}\text{Yb}(^1\text{S}_0)$ itinerant atoms and $^{171}\text{Yb}(^3\text{P}_2)$ localized impurities. In this case, the orbital angular momentum of the itinerant atoms is $I = \frac{1}{2}$, whereas the orbital angular momentum of the localized impurity atoms is $F = \frac{3}{2}$ [the electronic orbital moment is $J = 2$, and the nuclear spin is $I = \frac{1}{2}$]. The entropy and the specific heat in this case are given by eqs. (3.4) and (3.5) in Ref.⁴. Taking into account invariance of the entropy and the specific heat under the poor man's scaling, we get the following expressions,

$$S_{\text{s.d.}} = k_B \left\{ \ln(2F + 1) - \frac{\pi^2}{3} F(F + 1) \Lambda_{\text{s.d.}}^3(T) \right\}, \quad (63)$$

$$C_{\text{s.d.}} = k_B \pi^2 F(F + 1) \Lambda_{\text{s.d.}}^4(T), \quad (64)$$

where

$$\Lambda_d(T) = \frac{1}{\ln(T/T_K)}. \quad (65)$$

The entropy (63) and the specific heat (64) for the $^{171}\text{Yb}(^1\text{S}_0) - ^{171}\text{Yb}(^3\text{P}_2)$ system is shown in Fig. 9 [dashed curves in panels (a) and (b)].

B. Magnetic Susceptibility

In order to derive an expression for the magnetic susceptibility of the atomic gas with the Kondo impurity, we note that the itinerant atoms are in the electronic spin-singlet state, whereas the impurity is in the electronic spin-triplet state. Therefore interaction of itinerant atoms with the magnetic field is proportional to the nuclear magneton μ_n , whereas the interaction of the impurity with the magnetic field is proportional to the Bohr magneton μ_B . The interaction of the itinerant atoms and the impurity with the magnetic field $\mathbf{B} = B\mathbf{e}_z$ is described by the Hamiltonian,

$$H_B = -g_{\text{Yb}} \mu_n \sum_{i,i',\mathbf{k}} (\mathbf{B} \cdot \mathbf{I}_{i,i'}) c_{\mathbf{k},i}^\dagger c_{\mathbf{k},i'} - g \mu_B \sum_f (\mathbf{B} \cdot \mathbf{F}_{f,f'}) X^{f,f'}, \quad (66)$$

where $g_{\text{Yb}} = -0.2592$ is the nuclear g-factor of $^{173}\text{Yb}^{35}$, g is electronic g-factor of Yb atom in the $^3\text{P}_2$ state,

$$g = \frac{3J(J+1) + S(S+1) - L(L+1)}{2J(J+1)} = \frac{3}{2}, \quad (67)$$

where for the $^3\text{P}_2$ configuration, $J = 2$ and $L = S = 1$ [in this section, S and L denote the electronic spin and angular momentum of the $^{171}\text{Yb}(^3\text{P}_2)$ atom]. Then the impurity magnetization $\mathbf{M}_{\text{imp}} = M_{\text{imp}} \mathbf{e}_z$ can be written as⁴,

$$M_{\text{imp}} = g\mu_B \langle \hat{F}^z \rangle + g_{\text{Yb}} \mu_n \left\{ \langle \hat{I}^z \rangle - \langle \hat{I}^z \rangle_0 \right\}, \quad (68)$$

where $\langle \dots \rangle$ indicates a thermal average with respect to the total Hamiltonian $H + H_B$, and $\langle \dots \rangle_0$ with respect to $H_0 + H_B$,

$$\langle \mathcal{O} \rangle = \frac{\text{tr}(e^{-\beta(H+H_B)} \mathcal{O})}{\text{tr } e^{-\beta(H+H_B)}},$$

$$\langle \mathcal{O} \rangle_0 = \frac{\text{tr}(e^{-\beta(H_0+H_B)} \mathcal{O})}{\text{tr } e^{-\beta(H_0+H_B)}}.$$

Here H and H_0 are given by eq. (21).

The magnetic interaction described by the Hamiltonian (66) has a standard form of a scalar product of the external magnetic field and the magnetic dipole angular momentum operators of the impurity and itinerant atoms. It reflects the fact that (usually), only the dipole moment contributes to the linear magnetization of atoms. However, somewhat unexpectedly, the Kondo Hamiltonian (14) gives rise to nontrivial contributions of the quadrupole and octupole magnetic moments to the linear magnetization of the system. This requires an analysis that is distinct from the one the standard treatment

of magnetic susceptibility as applied to the $s-d$ Hamiltonian. In this section we derive the magnetic susceptibility as a function of temperature in the weak coupling regime, $T \gg T_K$.

C. Contributions to M_{imp} due to H_K

First, let us recall the expression for the magnetization of an isolated atom. To linear order in the magnetic field B , the magnetization of a single ^{173}Yb atom in the $^3\text{P}_2$ state with $F = \frac{3}{2}$ is,

$$M_{\text{imp}}^{(0)} = \frac{F(F+1)}{3T} (g\mu_B)^2 B. \quad (69)$$

Next, consider the contributions to M_{imp} due to H_K ,

$$\delta M_{\text{imp}} = M_{\text{imp}} - M_{\text{imp}}^{(0)}.$$

By definition, this contribution is given by,

$$\begin{aligned} \delta M_{\text{imp}} &= g\mu_B \left\{ \langle \hat{F}^z \rangle - \langle \hat{F}^z \rangle_0 \right\} + \\ &+ g_{\text{Yb}}\mu_n \left\{ \langle \hat{I}^z \rangle - \langle \hat{I}^z \rangle_0 \right\}. \end{aligned} \quad (70)$$

Assume that the couplings λ 's are small and expand δM_{imp} with powers of H_K ,

$$\delta M_{\text{imp}} = \sum_{n=1}^{\infty} \delta M_{\text{imp}}^{(n)}, \quad (71)$$

where $\delta M_{\text{imp}}^{(n)}$ is proportional to λ_{β}^n . Below we will calculate $\delta M_{\text{imp}}^{(1)}$ and $\delta M_{\text{imp}}^{(2)}$.

1. Corrections linear with λ 's

The correction $\delta M_{\text{imp}}^{(1)}$ can be written as,

$$\delta M_{\text{imp}}^{(1)} = \sum_{\beta} \left\{ \delta M_{\text{f};\beta} + \delta M_{\text{i};\beta} \right\}. \quad (72)$$

Here

$$\delta M_{\text{f};\beta} = -g\mu_B \int_0^{\beta} \left\langle \hat{F}^z H_{\beta}(\tau) \right\rangle_0 d\tau, \quad (73)$$

$$\delta M_{\text{i};\beta} = -g_{\text{Yb}}\mu_n \int_0^{\beta} \left\langle \hat{I}^z H_{\beta}(\tau) \right\rangle_0 d\tau, \quad (74)$$

where $\beta = \text{d}, \text{q}, \text{o}$ for dipole, quadrupole and octupole interactions, $H_{\text{d},\text{q},\text{o}}$ are given by eqs. (16), (17) and (18). The expectation values $\langle F^{\vec{\alpha}_{\beta}} \rangle$, $\langle I^{\vec{\alpha}_{\beta}} \rangle$, $\langle F^z F^{\vec{\alpha}_{\beta}} \rangle$ and $\langle I^z I^{\vec{\alpha}_{\beta}} \rangle$ [where $\hat{F}^{\vec{\alpha}_{\beta}}$ or $\hat{I}^{\vec{\alpha}_{\beta}}$ are dipole ($\beta = \text{d}$), quadrupole ($\beta = \text{q}$) and octupole ($\beta = \text{o}$) matrices for a localized impurity or

itinerant atoms, α 's are the Cartesian indices] are calculated in Appendix H. Then $\delta M_{\text{imp}}^{(1)}$ is,

$$\delta M_{\text{imp}}^{(1)} = -\frac{175B}{4T} g\mu_B g_{\text{Yb}}\mu_n \Lambda_{\text{d}}. \quad (75)$$

Note that the factor $\frac{175}{4}$ comes from,

$$\frac{2}{9} F(F+1) I(I+1)(2I+1) = \frac{175}{4}.$$

If instead of itinerant atoms with spin $I = \frac{5}{2}$, we use atoms with spin $s = \frac{1}{2}$, the last expression turns to

$$\frac{2}{9} F(F+1) s(s+1)(2s+1) = \frac{F(F+1)}{3},$$

which agrees with eq. (3.2) from Ref.⁴.

2. Corrections quadratic with λ 's

Calculating the second order correction, $\delta M_{\text{imp}}^{(2)}$, we get δM_{imp} up to λ^2 ,

$$\begin{aligned} \delta M_{\text{imp}} &= -M_{\text{imp}}^{(0)} N(I) \frac{g\mu_B}{g_{\text{Yb}}\mu_n} \times \\ &\times \left\{ \Lambda_{\text{d}} - \mathfrak{F}_{\text{d}}^{(2)} \ln \left(\frac{D}{T} \right) \right\}, \end{aligned} \quad (76)$$

where $M_{\text{imp}}^{(0)}$ is given by eq. (69), $N(I)$ is given by eq. (1), and

$$\mathcal{N}_I = \frac{2}{3} I(I+1)(2I+1), \quad (77)$$

$$\mathfrak{F}_{\text{d}}^{(2)} = -\Lambda_{\text{d}}^2 - \frac{9216}{25} \Lambda_{\text{q}}^2 - \frac{1469664}{25} \Lambda_{\text{o}}^2. \quad (78)$$

$\mathfrak{F}_{\text{d}}^{(2)}$ can be get from eq. (41a) neglecting the terms of order λ^3 .

The condition imposing the invariance of the magnetization under the poor mans scaling transformation is

$$\frac{\partial}{\partial \ln D} \left\{ \Lambda_{\text{d}} - \mathfrak{F}_{\text{d}}^{(2)} \ln \left(\frac{D}{T} \right) \right\} = 0. \quad (79)$$

Within the accuracy of this equation, when differentiating the second term, we should neglect any implicit dependence on D through the couplings Λ_{β} ($\beta = \text{d}, \text{q}, \text{o}$). The renormalization procedure should proceed until the bandwidth D is reduced to the temperature T . At this point, the second order of the perturbation theory vanishes and the magnetization takes the form,

$$M_{\text{imp}} = M_{\text{imp}}^{(0)} \left\{ 1 - \frac{g_{\text{Yb}}\mu_n}{g\mu_B} N(I) \Lambda_{\text{d}}(T) \right\}, \quad (80)$$

where $N(I)$ is given by eq. (1), $\Lambda_{\text{d}}(T)$ is the solution of the second order scaling equation (28).

It is useful to write the magnetic susceptibility $\chi_{\text{imp}} = \partial M_{\text{imp}} / \partial B$ as,

$$\chi_{\text{imp}}(T) = \chi_{\text{imp}}^{(0)} + \delta\chi_{\text{imp}}(T), \quad (81)$$

where $\chi_{\text{imp}}^{(0)}$ is the susceptibility of the isolated impurity atom, and $\delta\chi_{\text{imp}}(T)$ is correction to the susceptibility due to the Kondo interaction. Explicitly,

$$\chi_{\text{imp}}^{(0)} = \frac{\chi_0}{3} \frac{T_K}{T} F(F+1), \quad (82)$$

$$\delta\chi_{\text{imp}} = X_{\text{imp}} N(I) \Lambda_{\text{d}}, \quad (83)$$

where

$$\chi_0 = \frac{(g\mu_B)^2}{T_K}, \quad X_{\text{imp}} = -\frac{g_{\text{Yb}}\mu_n}{g\mu_B} \chi_{\text{imp}}^{(0)}.$$

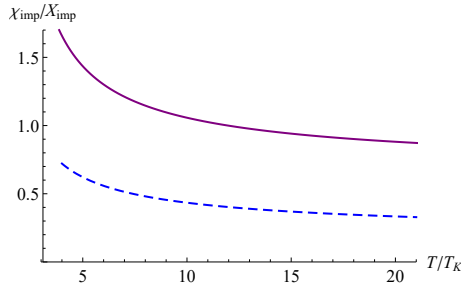


FIG. 10: (color online) Solid curve: The ratio $\delta\chi_{\text{imp}}/X_{\text{imp}}$ (83) as a function of T for $\lambda_0\rho_0 = 0.5$. The values of the parameters are $\Lambda_{\text{d}}^{(0)} = 0.0247619$, $\Lambda_{\text{q}}^{(0)} = -0.0005952$, $\Lambda_{\text{o}}^{(0)} = -0.0002646$. Dashed curve: The ratio $\delta\chi_{\text{s.d.}}/X_{\text{imp}}$ (84) for the $^{171}\text{Yb}({}^1\text{S}_0) - {}^{171}\text{Yb}({}^3\text{P}_2)$ system.

The ratio $\delta\chi_{\text{imp}}/X_{\text{imp}}$ as a function of temperature is shown in Fig. 10, solid curve. It should be noted that $X_{\text{imp}}/\chi_{\text{imp}}^{(0)} \ll 1$ since the ratio,

$$\frac{g_{\text{Yb}}\mu_n}{g\mu_B} = -9.411 \cdot 10^{-5},$$

is small. When T approaches the Kondo temperature, $\delta\chi_{\text{imp}}$ diverges as $1/\ln(T/T_K)$ which indicates breaking down of the underlying perturbation theory.

For comparison, consider a system consisting of $^{171}\text{Yb}({}^1\text{S}_0)$ itinerant atoms and a $^{171}\text{Yb}({}^3\text{P}_2)$ atom as localized impurity. The atomic orbital angular momentum is assumed to be $F = \frac{3}{2}$, therefore the susceptibility of the isolated impurity is given by eq. (82). Magnetic susceptibility of the $^{171}\text{Yb}({}^3\text{P}_2)$ atom interacting with the $^{171}\text{Yb}({}^1\text{S}_0)$ atoms [atomic orbital moment is $I = \frac{1}{2}$] is⁴,

$$\begin{aligned} \chi_{\text{s.d.}} &= \chi_{\text{imp}}^{(0)} + \delta\chi_{\text{s.d.}}, \\ \delta\chi_{\text{s.d.}} &= X_{\text{imp}} \Lambda_{\text{s.d.}}(T), \end{aligned} \quad (84)$$

where $\Lambda_{\text{s.d.}}(T)$ is given by eq. (65). The ratio $\delta\chi_{\text{s.d.}}/X_{\text{imp}}$, eq. (84), is shown in Fig. 10, dashed curve.

Experimental facets Having developed the theoretical framework for calculating a few thermodynamical quantities let us say a few words on the experimental aspects, specific for the task of measuring these thermodynamic quantities in the pertinent system. It is worth mentioning that some of these thermodynamic observables have been successfully measured in one-component Bose gases⁴³, two-component Fermi gases⁴⁴, and $\text{SU}(N)$ fermions trapped in optical lattices⁴⁵ either using *in-situ* local probe of the inhomogeneous atomic density^{44,46} or performing a spin transport measurements⁴⁷. In particular, the magnetic susceptibility of the two-component Fermi gas is determined in various ways, including (1) the relative spin fluctuation measurement⁴⁸, (2) the sum-rule approach for the spin-dipole mode frequency⁴⁷ or (3) the direct measurement of susceptibility from the inhomogeneous density profile of the spin-imbalanced atomic gas⁴⁹. Similar measurements should be feasible in a ${}^1\text{S}_0 - {}^3\text{P}_2$ ytterbium mixture. Indeed, the spin-dependent trapping potential available in the ytterbium mixture allows one to induce spin-selective transport and consequently monitor the spin-dipole mode of the system. In a similar manner, the heat capacity of the two-component gas can be determined from the local density of the atomic gas⁵⁰.

XI. CONCLUSION

Let us then briefly summarize our results. Our main arena concerns the Kondo physics in an ultracold Fermi gas of ^{173}Yb (${}^1\text{S}_0$) atoms (in their electronic ground-state) in which a few ^{173}Yb (${}^3\text{P}_2$) atoms (in a long lived excited state) are trapped in a specially designed optical potential. The main objectives are: 1) To explore the feasibility of experimental realization; 2) To calculate the exchange interaction between the itinerant $^{173}\text{Yb}({}^1\text{S}_0)$ and $^{173}\text{Yb}({}^3\text{P}_2)$ atoms and to verify that it is an antiferromagnetic exchange; 3) To construct the Kondo Hamiltonian and to identify its underlying symmetry; 4) To carry out the corresponding poor-man scaling, to identify the stable fixed points and to determine whether some of them display non-Fermi liquid behaviour; 5) To calculate some experimentally accessible observable in such a system.

As far as objective 1) is concerned, we have considered a mixture of ${}^1\text{S}_0$ and ${}^3\text{P}_2$ ytterbium fermions that can be readily prepared in a current experiment, in which a state-dependent optical potential using a strong ${}^3\text{P}_2 - {}^3\text{S}_1$ transition tightly confines ${}^3\text{P}_2$ atoms while makes ground-state ${}^1\text{S}_0$ atoms itinerant. By properly choosing the wavelength of the optical potential, we have shown that the spontaneous light scattering can be sufficiently reduced to observe a many-body effect. The localized and itinerant atoms can be then independently detected with the combination of optical pumping and blast. Finally a ${}^1\text{S}_0 - {}^3\text{P}_2$ mixture of ytterbium atoms has a magnetic Feshbach resonance by which the interaction strength between localized and itinerant atoms can be further controlled⁴¹. Such novel features may open a new route

to investigate the KE with tuneable atom-atom interactions in this system. Calculating the exchange interaction proceeds along similar lines as in our previous paper³¹.

The main difficulty is encountered in achieving goals (3) and (4). It is required to write down the Kondo Hamiltonian in terms of multiple expansion, since otherwise, the RG procedure is inapplicable. This requires a technically tedious procedure related to the pertinent spin algebra. Moreover, identifying the corresponding fixed points requires calculations of RG diagrams to third order in the exchange constant, which turn out to be rather involved. Details of the calculations are explained in the Appendices.

Having overcame these technical difficulties, we have found seven fixed points for λ_d and λ_q and λ_o . Three of them, P_4 , P_5 and P_7 [eqs. (42d), (42e) and (42g)] are stable, and the other fixed points are unstable. The fixed points found here are distinct from the NB non Fermi liquid fixed point described in our previous paper³¹, in which we studied the Kondo physics in a 1S_0 - 3P_0 mixture of ^{173}Yb atoms. In the present work, the NB non Fermi liquid fixed point corresponds to P_1 in the list (42d), and is *unstable*.

The remaining task, that is, elucidating the Kondo physics *in the strong coupling regime* for the new stable fixed points P_4 , P_5 and P_7 (identified here) is beyond the scope of our present study. It is perceived that the standard techniques that are applied to the dipolar KE such as Bethe Ansatz and conformal field theory might work also in this case albeit with non-trivial modifications.

Acknowledgement

Y.A, I.K and T.K acknowledge many years of collaboration and discussions pertaining to the Kondo Physics with their colleague and their close friend

Konstantin Abramovich Kikoin.

His sudden death left us shocked and wordless.

The authors thank S. Zhang for useful discussion. G.B.J acknowledges financial support from the Hong Kong Research Grants Council (Project No. 26300014/16300215/16311516) and from the Croucher Foundation. The research of Y.A is partially supported by grant 400/12 of the Israeli Science Foundation.

Appendix A: Trapping of the Yb Atoms by the Optical Potential

Since the $\text{Yb}({}^3\text{P}_2)$ atom has the electronic orbital moment $J = 2$, the polarizability $\hat{\alpha}_e(\omega)$ is a 5×5 matrix. We introduce the matrices $\hat{\alpha}_e^x(\omega)$, $\hat{\alpha}_e^y(\omega)$ and $\hat{\alpha}_e^z(\omega)$, for the electric field collinear to the axes x , y and z , respectively. Explicitly, they are

$$\begin{aligned} \hat{\alpha}_e^z &= \text{diag}(\alpha_2, \alpha_1, \alpha_0, \alpha_1, \alpha_2), \\ \hat{\alpha}_e^\beta &= \hat{\mathcal{U}}_\beta \hat{\alpha}_e^z \hat{\mathcal{U}}_\beta^\dagger, \end{aligned} \quad (\text{A1})$$

where $\beta = x, y$ is a Cartesian index, the spin-rotation matrices $\hat{\mathcal{U}}_\beta$ are

$$\hat{\mathcal{U}}_x = e^{i\pi\hat{J}^x/2}, \quad \hat{\mathcal{U}}_y = e^{-i\pi\hat{J}^y/2}.$$

We consider the optical potential generated by standing electromagnetic wave in the directions of the axes x, y and z with the double-magic wavelength λ_0 ³³,

$$\lambda_0 = 546 \text{ nm}. \quad (\text{A2})$$

The polarizability $\hat{\alpha}_F^\beta(\omega_h) = \alpha_e(\lambda_0)\hat{J}^0$ [the Cartesian index β indicates the direction of the electric field] is proportional to the identity matrix \hat{J}^0 . Explicitly, $\alpha_g(\lambda_0)$ and $\alpha_e(\lambda_0)$, the polarizability of the $\text{Yb}({}^1\text{S}_0)$ and $\text{Yb}({}^3\text{P}_2)$ atoms are³³

$$\alpha_e(\omega_h) = 250 \text{ a.u.}, \quad \alpha_g(\omega_h) = 200 \text{ a.u.} \quad (\text{A3})$$

1. Optical Potential

We consider possibility of formation of the short- and long-length potentials the light of the double-magic wavelength λ_0 . The optical potential is generated by three pairs of lasers, as illustrated in Fig. 11. The light of the first, second or third pair of lasers propagates parallel and antiparallel to the axes x , y or z . The optical potential is,

$$V_\nu(\mathbf{r}) = -\alpha_\nu(\omega) \lim_{\mathcal{T} \rightarrow \infty} \frac{1}{\mathcal{T}} \int_0^{\mathcal{T}} |\mathbf{E}(\mathbf{r}, t)|^2 dt, \quad (\text{A4})$$

where $\nu = g$ or e for the $\text{Yb}({}^1\text{S}_0)$ or $\text{Yb}({}^3\text{P}_2)$ atoms. The electric field $\mathbf{E}(\mathbf{r})$ is,

$$\mathbf{E}(\mathbf{r}, t) = \sum_{\beta=1}^6 \mathbf{E}_\beta(\mathbf{r}, t). \quad (\text{A5})$$

Here

$$\begin{aligned} \mathbf{E}_\beta(\mathbf{r}, t) &= \mathbf{E}_\beta^{(0)} \cos(\mathbf{k}_\beta \mathbf{r} - \omega_0 t) \times \\ &\times \exp\left(-\frac{x_{a_\beta}^2 - x_{b_\beta}^2}{2L^2}\right), \end{aligned} \quad (\text{A6})$$

where $\mathbf{E}_\beta^{(0)} = E_u \mathbf{e}_{a_\beta}$, $\mathbf{E}_{\beta+3}^{(0)} = E_v \mathbf{e}_{a_\beta}$, $\beta = 1, 2, 3$. The indices $a_\beta = a_{\beta+3}$ and $b_\beta = b_{\beta+3}$ are

$$\begin{aligned} a_1 &= 2, & a_2 &= 3, & a_3 &= 1, \\ b_1 &= 3, & b_2 &= 1, & b_3 &= 2. \end{aligned} \quad (\text{A7})$$

\mathbf{e}_1 , \mathbf{e}_2 and \mathbf{e}_3 are unit vectors parallel to the axes x , y and z . The amplitudes E_u and E_v are real and satisfy the inequalities

$$E_u \gg E_v > 0.$$

The wave vectors of the light are $\mathbf{k}_\beta = -\mathbf{k}_{\beta+3} = k_0 \mathbf{e}_\beta$, where $\beta = 1, 2, 3$, $k_0 = 2\pi_0/\lambda_0$ is the wavenumber of the

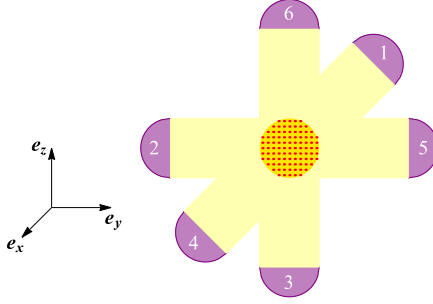


FIG. 11: (Color online) Three pairs of lasers labelled by the numbers 1 – 6 generating trapping optical potential [golden yellow disk with red dots].

light. $\omega_0 = k_0 c$ is the frequency of the light. The waist radius $2L$ satisfies the inequality

$$k_0 L \gg 1.$$

Explicitly, the optical potential is

$$V_\nu(\mathbf{r}) = V_\nu^{(\text{slow})}(\mathbf{r}) + V_\nu^{(\text{fast})}(\mathbf{r}). \quad (\text{A8})$$

Here

$$V_\nu^{(\text{slow})}(\mathbf{r}) = \sum_{\beta=1}^3 V_{\beta,\nu}^{(\text{slow})}(\mathbf{r}), \quad (\text{A9})$$

$$V_\nu^{(\text{fast})}(\mathbf{r}) = \sum_{\beta=1}^3 V_{\beta,\nu}^{(\text{fast})}(\mathbf{r}), \quad (\text{A10})$$

where

$$V_{\beta,\nu}^{(\text{slow})}(\mathbf{r}) = -V_{0,\nu} \exp\left(-\frac{x_{a_\beta}^2 + x_{b_\beta}^2}{L^2}\right), \quad (\text{A11})$$

$$V_{\beta,\nu}^{(\text{fast})}(\mathbf{r}) = -V_{1,\nu} \cos(2k_0 x_\beta) \times \exp\left(-\frac{x_{a_\beta}^2 + x_{b_\beta}^2}{L^2}\right). \quad (\text{A12})$$

The strengths $V_{0,\nu}$ and $V_{1,\nu}$ are

$$V_{0,\nu} = \frac{\alpha_\nu(\omega_0)}{2} \left\{ E_u^2 + E_v^2 \right\},$$

$$V_{1,\nu} = \alpha_\nu(\omega_0) E_u E_v.$$

We assume that E_u and E_v are real and positive and $\alpha_\nu(\lambda_0) > 0$, and therefore $V_{0,\nu} > 0$ and $V_{1,\nu} > 0$. Here β is a Cartesian index, the indices a_β and b_β are given by eq. (A7).

The optical potential (A8) is illustrated in Fig. 12 for $L = 10\lambda_0$ and $E_v = 0.05E_u$. Here the solid blue and green curves show $V_\nu(x, 0, 0)$ and $V_\nu(x, \lambda_0/4, \lambda_0/4)$. For comparison, the dashed red curve illustrates $V_\nu^{(\text{slow})}(x, 0, 0)$, eq. (A9). Note that we take here $L = 10\lambda_0$ just for better illustration. Real values of L are larger than $10^2\lambda_0$.

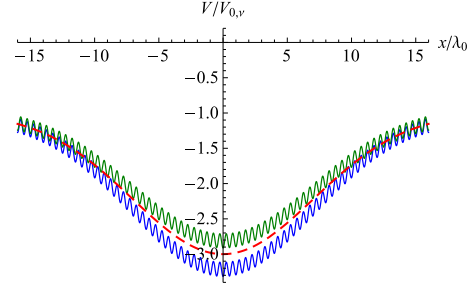


FIG. 12: (Color online) $V_\nu(x, 0, 0)$ [solid blue curve], $V_\nu(x, \lambda_0/4, \lambda_0/4)$ [solid green curve] and $V_\nu^{(\text{slow})}(x, 0, 0)$ [dashed red curve] as functions of x for $L = 10\lambda_0$ and $E_v = 0.05E_u$.

In the following discussions, we assume that the Yb^3P_2 atoms are trapped by the fast oscillating potential (A10) and are localized near the stable equilibrium points $\mathbf{r} = (n_1\lambda_0/2, n_2\lambda_0/2, n_3\lambda_0/2)$, where n_1, n_2 and n_3 are integers. From the other side, we assume that the density of the Yb^1S_0 atoms is such that the Fermi energy ϵ_F [measured from the bottom of the potential well] satisfies the inequality $\epsilon_F \gg V_{1,g}$, and therefore the atoms with energy close to ϵ_F can be considered as itinerant: their motion is restricted by the potential $V_g^{(\text{slow})}(\mathbf{r})$, eq. (A9).

2. Wave Function and Energy of the Trapped Yb^3P_2 Atoms

The density of the Yb^3P_2 atoms are low, so that all the atoms are localized by the fast oscillating potential (A10). When the energy level of the atom is deep enough, we can derive the wave function and the energy level in harmonic approximation. Consider, for example, the atom trapped near the stable equilibrium point $\mathbf{r} = (0, 0, 0)$. When the radius of localization of the atom is small with respect to $\lambda_0/4$, the optical potential (A10) can be approximated as,

$$V_e^{(\text{fast})}(\mathbf{r}) \approx -V_{1,e} + 2V_{1,e} (k_0 r)^2, \quad (\text{A13})$$

whereas $V_e^{(\text{slow})}(\mathbf{r})$ is almost constant for $r < \lambda_0/4$, where $r = |\mathbf{r}|$. The wave function of the atom trapped by the harmonic potential (A13) is,

$$\Psi_e(r) = \frac{1}{(\pi a_e^2)^{3/4}} \exp\left(-\frac{r^2}{2a_e^2}\right). \quad (\text{A14})$$

The harmonic length and frequency are,

$$k_0 a_e = \left(\frac{\mathcal{E}_0}{2V_{1,e}}\right)^{\frac{1}{4}}, \quad \hbar\Omega_e = 2\sqrt{2\mathcal{E}_0 V_{1,e}}, \quad (\text{A15})$$

where the recoil energy \mathcal{E}_0 is

$$\mathcal{E}_0 = \frac{\hbar^2 k_0^2}{2M}, \quad (\text{A16})$$

where M is the atomic mass.

The energy ε_{imp} measured from the bottom of the well is,

$$\varepsilon_{\text{imp}} = \frac{3}{2} \hbar \Omega_e. \quad (\text{A17})$$

3. Wave Functions and Energy Levels of the Trapped $\text{Yb}({}^1\text{S}_0)$ Atoms

When the energy ϵ of the trapped $\text{Yb}({}^1\text{S}_0)$ atom [measured from the bottom of the potential well] satisfies the inequality $\epsilon \gg V_{1,g}$, we can approximate the potential (A8) as

$$V_g(\mathbf{r}) \approx V_g^{(\text{slow})}(\mathbf{r}). \quad (\text{A18})$$

Moreover, when the energy level is deep enough, we can approximate $V_g^{(\text{slow})}(\mathbf{r})$ as,

$$V_g^{(\text{slow})}(\mathbf{r}) \approx -3V_{0,g} + 2V_{0,g} \frac{r^2}{L^2}. \quad (\text{A19})$$

Quantum states of atoms in isotropic potential are described by the radial quantum number n [$n = 0, 1, 2, \dots$], the angular momentum L [$L = 0, 1, 2, \dots$] and projection m of the angular momentum on the axis z [$m = -L, -L+1, \dots, L$]. Due to the centrifugal barrier, only the atoms with $L = 0$ can approach the impurity and be involved in the exchange interaction with it. The wave functions of the atoms with $L = 0$ trapped by the harmonic potential (A19) are,

$$\Psi_n(\mathbf{r}) = \frac{\mathcal{N}_n}{\sqrt{4\pi}} L_n^{(\frac{1}{2})} \left(\frac{r^2}{a_g^2} \right) \exp \left(-\frac{r^2}{2a_g^2} \right), \quad (\text{A20})$$

where $L_n^{(\frac{1}{2})}(\varrho)$ are generalized Laguerre polynomials. The normalization factor is

$$\mathcal{N}_n = \left(\frac{2}{\pi a_g^6} \right)^{1/4} \sqrt{\frac{2^{n+2} n!}{(2n+1)!!}}.$$

The harmonic length a_g and frequency Ω_g are defined as

$$\frac{a_g}{L} = \left(\frac{\mathcal{E}_L}{2V_{0,g}} \right)^{1/4}, \quad \hbar \Omega_g = 2\sqrt{2\mathcal{E}_L V_{0,g}}, \quad (\text{A21})$$

where \mathcal{E}_L is defined as,

$$\mathcal{E}_L = \frac{\hbar^2}{2ML^2}. \quad (\text{A22})$$

The energy levels of the states with $L = 0$ are,

$$\varepsilon_n = \hbar \Omega_g \left(2n + \frac{3}{2} \right). \quad (\text{A23})$$

In what following we assume that

$$\Omega_e \gg \Omega_g. \quad (\text{A24})$$

Within this framework, the spectrum is nearly continuous and the ytterbium atoms in the ground-state form a Fermi gas. The Fermi energy ϵ_F is such that $\epsilon_F \gg \hbar \Omega_g$, hence the Fermi gas is 3D.

Appendix B: Exchange Interaction

Appendices B, C, D, E main points: The second order correction terms are defined in Eqs. (26, 27), while the third ordered correction terms are defined in Eqs. (35). The formidable task of evaluating these terms is carried out in these subsections.

When an impurity atom is localized at the origin of coordinates and an itinerant atom is placed at position \mathbf{R} so that they are separated by $R = |\mathbf{R}|$, there is an exchange interaction between them. The interaction Hamiltonian is,

$$\mathcal{H}_{\text{exch}}(R) = \sum_{f,f'} \sum_{i,i'} V_{f,f';i,i'}(R) \times X^{f,f'} \hat{\psi}_{i'}^\dagger(\mathbf{R}) \hat{\psi}_i(\mathbf{R}), \quad (\text{B1})$$

where $X^{f,f'} = |f\rangle\langle f'|$ are Hubbard operators of the localized impurity, $\hat{\psi}_i(\mathbf{R})$ and $\hat{\psi}_{i'}^\dagger(\mathbf{R})$ are annihilation and creation operators of itinerant atoms at position \mathbf{R} with the nuclear magnetic quantum number i . The rate $V_{f,f';i,i'}(R)$ is,

$$V_{f,f';i,i'}(R) = \frac{t_s(R) t_p(R)}{3 \Delta \epsilon} \sum_j C_{J,j;I,i}^{F,f} C_{J,j;I,i'}^{F,f'} \quad (\text{B2})$$

Here $t_s(R)$ and $t_p(R)$ are given by eq. (11),

$$\Delta \epsilon = \varepsilon_{\text{ion}} + \varepsilon_{\text{ea}} + \epsilon_g - \epsilon_x = 4.1104 \text{ eV},$$

where $\varepsilon_{\text{ion}} = 6.2542 \text{ eV}$ is the ionization energy³⁷, $\varepsilon_{\text{ea}} = 0.3 \text{ eV}$ is the electron affinity³⁸ and $\epsilon_x - \epsilon_g = 2.4438 \text{ eV}$ is the excitation energy of the ${}^3\text{P}_2$ state³⁷.

Substituting eq. (B2) into eq. (B1), we get

$$\mathcal{H}_{\text{exch}}(R) = g(R) \sum_j \sum_{f,f'} \sum_{i,i'} C_{J,j;I,i}^{F,f} C_{J,j;I,i'}^{F,f'} \times X^{f,f'} \hat{\psi}_{i'}^\dagger(\mathbf{R}) \hat{\psi}_i(\mathbf{R}), \quad (\text{B3})$$

where

$$g(R) = \frac{t_s(R) t_p(R)}{3 \Delta \epsilon}. \quad (\text{B4})$$

Appendix C: Derivation of $\delta H_{\beta,\beta'}^{(2)}$, Eq. (27)

Here we consider in turn the various multiple contributions to $\delta H_{\beta,\beta'}^{(2)}$ with $\beta, \beta' = \text{d, q, o}$.

1. Dipole-dipole contribution: The correction $\delta H_{\text{d,d}}^{(2)}$ [eq. (27)] is,

$$\begin{aligned} \delta H_{\text{d,d}}^{(2)} = & -\frac{\lambda_{\text{d}}^2}{D} \frac{k_F^2}{a_g^4} \sum_{\alpha,\alpha'} \sum_{f,f',f''} \sum_{i,i',i''} \sum_{n,n',n''} F_{f,f''}^\alpha F_{f'',f'}^{\alpha'} \times \\ & \times X^{f,f'} c_{n,i}^\dagger c_{n',i'} \left(I_{i,i''}^\alpha I_{i'',i'}^{\alpha'} \langle c_{n'',i''} c_{n'',i''}^\dagger \rangle - \right. \\ & \left. - I_{i,i''}^{\alpha'} I_{i'',i'}^\alpha \langle c_{n'',i''}^\dagger c_{n'',i''} \rangle \right). \end{aligned} \quad (\text{C1})$$

Here the energy of atoms with harmonic quantum numbers n, n' belong to the reduced energy band, whereas the energy of atoms with the harmonic quantum number n'' is located near the edge of the energy band such that

$$|\varepsilon_n|, |\varepsilon_{n'}| < D', \quad D' < |\varepsilon_{n''}| < D,$$

where $D > D' = D - \delta D$. When $D' \gg T$ (T is the temperature of the gas), we can write

$$\begin{aligned} \langle c_{n'',i''} c_{n'',i''}^\dagger \rangle &= \Theta(\varepsilon_{n''} - D) \Theta(-D' - \varepsilon_{n''}), \\ \langle c_{n'',i''}^\dagger c_{n'',i''} \rangle &= \Theta(\varepsilon_{n''} - D') \Theta(D - \varepsilon_{n''}), \end{aligned}$$

where $\Theta(\epsilon)$ is the Heaviside theta function equal to 1 for $\epsilon > 0$, 0 for $\epsilon < 0$ and $\frac{1}{2}$ for $\epsilon = 0$. Thus, the correction $H_{d,d}^{(2)}$ can be written as,

$$\begin{aligned} \delta H_{d,d}^{(2)} &= -\frac{\lambda_d^2 \rho_0 \delta D}{2D} \frac{k_F^2}{a_g^4} \sum_{\alpha,\alpha'} \sum_{f,f'} \sum_{i,i'} \sum_{n,n'} \left[\hat{F}^\alpha, \hat{F}^{\alpha'} \right]_{f,f'} \times \\ &\quad \times \left[\hat{I}^\alpha, \hat{I}^{\alpha'} \right]_{i,i'} X^{f,f'} c_{n,i}^\dagger c_{n',i'}, \end{aligned} \quad (C2)$$

where

$$[\hat{A}, \hat{B}] = \hat{A}\hat{B} - \hat{B}\hat{A},$$

denotes the commutator of the matrices \hat{A} and \hat{B} . ρ_0 is the density of states of itinerant atoms. Taking into account the property of the Levi-Civita symbols,

$$\sum_{\alpha,\alpha'} \epsilon^{\alpha,\alpha',\alpha_1} \epsilon^{\alpha,\alpha',\alpha'_1} = 2 \delta^{\alpha_1,\alpha'_1}, \quad (C3)$$

we get,

$$\begin{aligned} \delta H_{d,d}^{(2)} &= \frac{\lambda_d^2 \rho_0 \delta D}{D} \frac{k_F^2}{a_g^4} \sum_{\alpha} \sum_{f,f'} \sum_{i,i'} \sum_{n,n'} F_{f,f'}^\alpha I_{i,i'}^\alpha \times \\ &\quad \times X^{f,f'} c_{n,i}^\dagger c_{n',i'}. \end{aligned} \quad (C4)$$

2. Dipole-quadrupole contribution: The correction $\delta H_{d,q}^{(2)}$ [eq. (27)] is,

$$\begin{aligned} \delta H_{d,q}^{(2)} &= -\frac{\lambda_d \lambda_q \rho_0 \delta D}{2D} \frac{k_F^2}{a_g^4} \sum_{\alpha_1,\alpha_2,\alpha'_2} \sum_{f,f'} \sum_{i,i'} \sum_{n,n'} \times \\ &\quad \times \left[\hat{F}^{\alpha_1}, \hat{F}^{\alpha_2, \alpha'_2} \right]_{f,f'} \left[\hat{I}^{\alpha_1}, \hat{I}^{\alpha_2, \alpha'_2} \right]_{i,i'} \times \\ &\quad \times X^{f,f'} c_{n,i}^\dagger c_{n',i'}, \end{aligned} \quad (C5)$$

where ρ_0 is the density of states (25) of itinerant atoms. Taking into account the property (C3) of the Levi-Civita symbols, we get

$$\begin{aligned} \delta H_{d,q}^{(2)} &= \frac{6\lambda_d \lambda_q \rho_0 \delta D}{D} \frac{k_F^2}{a_g^4} \sum_{\alpha,\alpha'} \sum_{f,f'} \sum_{i,i'} \sum_{n,n'} F_{f,f'}^{\alpha,\alpha'} I_{i,i'}^{\alpha,\alpha'} \times \\ &\quad \times X^{f,f'} c_{n,i}^\dagger c_{n',i'}. \end{aligned} \quad (C6)$$

3. Dipole-octupole contribution: The correction $\delta H_{d,o}^{(2)}$ [eq. (27)] is,

$$\begin{aligned} \delta H_{d,o}^{(2)} &= -\frac{\lambda_d \lambda_o \rho_0 \delta D}{2D} \frac{k_F^2}{a_g^4} \sum_{\alpha_1} \sum_{\alpha_2,\alpha'_2,\alpha''_2} \sum_{f,f'} \sum_{i,i'} \sum_{n,n'} \times \\ &\quad \times \left[\hat{F}^{\alpha_1}, \hat{F}^{\alpha_2, \alpha'_2, \alpha''_2} \right]_{f,f'} \left[\hat{I}^{\alpha_1}, \hat{I}^{\alpha_2, \alpha'_2, \alpha''_2} \right]_{i,i'} \times \\ &\quad \times X^{f,f'} c_{n,i}^\dagger c_{n',i'}, \end{aligned} \quad (C7)$$

where ρ_0 is the density of states (25) of itinerant atoms. Taking into account the property (C3) of the Levi-Civita symbols, we get

$$\begin{aligned} \delta H_{d,o}^{(2)} &= \frac{9\lambda_d \lambda_o \rho_0 \delta D}{D} \frac{k_F^2}{a_g^4} \sum_{\alpha,\alpha',\alpha''} \sum_{f,f'} \sum_{i,i'} \sum_{n,n'} \times \\ &\quad \times F_{f,f'}^{\alpha,\alpha',\alpha''} I_{i,i'}^{\alpha,\alpha',\alpha''} X^{f,f'} c_{n,i}^\dagger c_{n',i'}. \end{aligned} \quad (C8)$$

4. Quadrupole-quadrupole contribution: The correction $\delta H_{q,q}^{(2)}$ [eq. (27)] is,

$$\begin{aligned} \delta H_{q,q}^{(2)} &= -\frac{\lambda_q^2 \rho_0 \delta D}{2D} \frac{k_F^2}{a_g^4} \sum_{\alpha_1,\alpha'_1} \sum_{\alpha_2,\alpha'_2} \sum_{f,f'} \sum_{i,i'} \sum_{n,n'} \times \\ &\quad \times \left[\hat{F}^{\alpha_1, \alpha'_1}, \hat{F}^{\alpha_2, \alpha'_2} \right]_{f,f'} \left[\hat{I}^{\alpha_1, \alpha'_1}, \hat{I}^{\alpha_2, \alpha'_2} \right]_{i,i'} \times \\ &\quad \times X^{f,f'} c_{n,i}^\dagger c_{n',i'}, \end{aligned} \quad (C9)$$

where ρ_0 is the density of states (25) of itinerant atoms. Taking into account the property (C3) of the Levi-Civita symbols, we get

$$\begin{aligned} \delta H_{q,q}^{(2)} &= \frac{64\lambda_q^2 \rho_0 \delta D}{9D} \frac{k_F^2}{a_g^4} \sum_{\alpha,\alpha',\alpha''} \sum_{f,f'} \sum_{i,i'} \sum_{n,n'} \times \\ &\quad \times F_{f,f'}^{\alpha,\alpha',\alpha''} I_{i,i'}^{\alpha,\alpha',\alpha''} X^{f,f'} c_{n,i}^\dagger c_{n',i'} + \\ &+ \frac{9216\lambda_q^2 \rho_0 \delta D}{25D} \frac{k_F^2}{a_g^4} \sum_{\alpha} \sum_{f,f'} \sum_{i,i'} \sum_{n,n'} \times \\ &\quad \times F_{f,f'}^{\alpha} I_{i,i'}^{\alpha} X^{f,f'} c_{n,i}^\dagger c_{n',i'}. \end{aligned} \quad (C10)$$

5. Quadrupole-octupole contribution: The correction $\delta H_{q,o}^{(2)}$ [eq. (27)] is,

$$\begin{aligned} \delta H_{q,o}^{(2)} &= -\frac{\lambda_q \lambda_o \rho_0 \delta D}{2D} \frac{k_F^2}{a_g^4} \sum_{\alpha_1,\alpha'_1} \sum_{\alpha_2,\alpha'_2,\alpha''_2} \sum_{f,f'} \sum_{i,i'} \sum_{n,n'} \times \\ &\quad \times \left[\hat{F}^{\alpha_1, \alpha'_1}, \hat{F}^{\alpha_2, \alpha'_2, \alpha''_2} \right]_{f,f'} \times \\ &\quad \times \left[\hat{I}^{\alpha_1, \alpha'_1}, \hat{I}^{\alpha_2, \alpha'_2, \alpha''_2} \right]_{i,i'} \times \\ &\quad \times X^{f,f'} c_{n,i}^\dagger c_{n',i'}, \end{aligned} \quad (C11)$$

where ρ_0 is the density of states (25) of itinerant atoms. Then eq. (C11) takes the form,

$$\begin{aligned} \delta H_{q,o}^{(2)} &= \frac{1458\lambda_q \lambda_o}{D_0} \frac{k_F^2}{a_g^4} \sum_{\alpha,\alpha'} \sum_{f,f'} \sum_{i,i'} \sum_{n,n'} F_{f,f'}^{\alpha,\alpha'} I_{i,i'}^{\alpha',\alpha} \times \\ &\quad \times X^{f,f'} c_{n',i'}^\dagger c_{n,i}. \end{aligned} \quad (C12)$$

6. Octuple-octuple contribution: The correction $\delta H_{\text{o},\text{o}}^{(2)}$ [eq. (27)] is,

$$\begin{aligned} \delta H_{\text{o},\text{o}}^{(2)} = & -\frac{\lambda_{\text{q}}\lambda_{\text{o}}\rho_0\delta D}{2D} \frac{k_F^2}{a_{\text{g}}^4} \sum_{\alpha_1,\alpha'_1,\alpha''_1} \sum_{\alpha_2,\alpha'_2,\alpha''_2} \sum_{f,f'} \sum_{i,i'} \sum_{n,n'} \\ & \times \left[\hat{F}^{\alpha_1,\alpha'_1,\alpha''_1}, \hat{F}^{\alpha_2,\alpha'_2,\alpha''_2} \right]_{f,f'} \times \\ & \times \left[\hat{I}^{\alpha_1,\alpha'_1,\alpha''_1}, \hat{I}^{\alpha_2,\alpha'_2,\alpha''_2} \right]_{i,i'} \times \\ & \times X^{f,f'} c_{n,i}^\dagger c_{n',i'}, \end{aligned} \quad (\text{C13})$$

where ρ_0 is the density of states (25) of itinerant atoms. Then eq. (C13) takes the form,

$$\begin{aligned} \delta H_{\text{o},\text{o}}^{(2)} = & \frac{1469664\lambda_{\text{o}}^2\rho_0}{D_0} \frac{k_F^2}{a_{\text{g}}^4} \sum_{\alpha} \sum_{f,f'} \sum_{i,i'} \sum_{n,n'} F_{f,f'}^\alpha I_{i',i}^\alpha \times \\ & \times X^{f,f'} c_{n',i'}^\dagger c_{n,i} - \\ & - \frac{306\lambda_{\text{o}}^2\rho_0}{5} \frac{k_F^2}{a_{\text{g}}^4} \sum_{\alpha,\alpha',\alpha''} \sum_{f,f'} \sum_{i,i'} \sum_{n,n'} \times \\ & \times F_{f,f'}^{\alpha,\alpha',\alpha''} I_{i',i}^{\alpha'',\alpha',\alpha} X^{f,f'} c_{n',i'}^\dagger c_{n,i}. \end{aligned} \quad (\text{C14})$$

Appendix D: Derivation of δE , Eq. (33)

The second order correction to the energy is illustrated by the diagrams displayed in Fig. 5. is decomposed into its multiple components as,

$$\delta E = \delta E_{\text{d}} + \delta E_{\text{q}} + \delta E_{\text{o}}. \quad (\text{D1})$$

Here δE_{d} , δE_{q} and δE_{o} are dipole, quadrupole and octuple contributions to δE , given explicitly as,

$$\begin{aligned} \delta E_{\text{d}} = & -\lambda_{\text{d}}^2 \frac{E}{D^2} \frac{k_F^2}{a_{\text{g}}^4} \sum_{f,f'} X^{f,f'} \sum_{\alpha_1,\alpha_2} \left(\hat{F}^{\alpha_1} \hat{F}^{\alpha_2} \right)_{f,f'} \times \\ & \times \text{Tr} \left(\hat{I}^{\alpha_1} \hat{I}^{\alpha_2} \right) \mathfrak{G}, \end{aligned} \quad (\text{D2a})$$

$$\begin{aligned} \delta E_{\text{q}} = & -\lambda_{\text{q}}^2 \frac{E}{D^2} \frac{k_F^2}{a_{\text{g}}^4} \sum_{f,f'} X^{f,f'} \times \\ & \times \sum_{\alpha_1,\alpha'_1} \sum_{\alpha_2,\alpha'_2} \left(\hat{F}^{\alpha_1,\alpha'_1} \hat{F}^{\alpha_2,\alpha'_2} \right)_{f,f'} \times \\ & \times \text{Tr} \left(\hat{I}^{\alpha_1,\alpha'_1} \hat{I}^{\alpha_2,\alpha'_2} \right) \mathfrak{G}, \end{aligned} \quad (\text{D2b})$$

$$\begin{aligned} \delta E_{\text{o}} = & -\lambda_{\text{o}}^2 \frac{E}{D^2} \frac{k_F^2}{a_{\text{g}}^4} \sum_{f,f'} X^{f,f'} \sum_{\alpha_1,\alpha'_1,\alpha''_1} \sum_{\alpha_2,\alpha'_2,\alpha''_2} \times \\ & \times \left(\hat{F}^{\alpha_1,\alpha'_1,\alpha''_1} \hat{F}^{\alpha_2,\alpha'_2,\alpha''_2} \right)_{f,f'} \times \\ & \times \text{Tr} \left(\hat{I}^{\alpha_1,\alpha'_1,\alpha''_1} \hat{I}^{\alpha_2,\alpha'_2,\alpha''_2} \right) \mathfrak{G}, \end{aligned} \quad (\text{D2c})$$

where \mathfrak{G} is given by eq. (36). We consider dipole, quadrupole and octuple contributions to δE in turn.

1. Dipole contribution: The trace of the product of two spin matrices is,

$$\sum_{i_1,i_2} I_{i_1,i_2}^{\alpha_1} I_{i_2,i_1}^{\alpha_2} = \frac{1}{3} I(I+1)(2I+1) \delta^{\alpha_1,\alpha_2}. \quad (\text{D3})$$

Using eq. (D3), we can write

$$\sum_{\alpha} \sum_{f_1} F_{f,f_1}^{\alpha} F_{f_1,f'}^{\alpha} = F(F+1) \delta_{f,f'}. \quad (\text{D4})$$

Finally, the dipole contribution to the self energy is,

$$\delta E_{\text{d}} = -\frac{2\delta D}{3D} E \Lambda_{\text{d}}^2 F(F+1)I(I+1)(2I+1).$$

Taking into account that $F = \frac{3}{2}$ and $I = \frac{5}{2}$, we get

$$\delta E_{\text{d}} = -\frac{525}{4} \frac{\delta D}{D} E \Lambda_{\text{d}}^2. \quad (\text{D5})$$

2. Quadrupole contribution: The trace of the product of two quadrupole matrices is,

$$\begin{aligned} \sum_{i_1,i_2} I_{i_1,i_2}^{\alpha_1,\alpha'_1} I_{i_2,i_1}^{\alpha_2,\alpha'_2} = & -\frac{112}{3} \left\{ 2 \delta_{\alpha_1,\alpha'_1} \delta_{\alpha_2,\alpha'_2} - \right. \\ & \left. - 3 [\delta_{\alpha_1,\alpha_2} \delta_{\alpha'_1,\alpha'_2} + \delta_{\alpha_1,\alpha'_2} \delta_{\alpha'_1,\alpha_2}] \right\}. \end{aligned} \quad (\text{D6})$$

Using eq. (D6), we can write

$$\begin{aligned} \sum_{\alpha_1,\alpha'_1} \sum_{\alpha_2,\alpha'_2} \hat{F}^{\alpha_1,\alpha'_1} \hat{F}^{\alpha_2,\alpha'_2} \text{Tr} \left(\hat{I}^{\alpha_1,\alpha'_1} \hat{I}^{\alpha_2,\alpha'_2} \right) = \\ = 6720 \hat{1}_4, \end{aligned} \quad (\text{D7})$$

where $\hat{1}_4$ is the 4×4 identity matrix.

Finally, quadrupole contribution to the self energy is,

$$\delta E_{\text{q}} = -13440 \frac{\delta D}{D} E \Lambda_{\text{q}}^2. \quad (\text{D8})$$

3. Octupole contribution: The trace of the product of two quadrupole matrices is,

$$\begin{aligned} \sum_{\alpha_1,\alpha'_1,\alpha''_1} \sum_{\alpha_2,\alpha'_2,\alpha''_2} \hat{F}^{\alpha_1,\alpha'_1,\alpha''_1} \hat{F}^{\alpha_2,\alpha'_2,\alpha''_2} \times \\ \times \text{Tr} \left(\hat{I}^{\alpha_1,\alpha'_1,\alpha''_1} \hat{I}^{\alpha_2,\alpha'_2,\alpha''_2} \right) = 1653372 \hat{1}_4, \end{aligned} \quad (\text{D9})$$

where $\hat{1}_4$ is the 4×4 identity matrix.

Finally, octupole contribution to the self energy is,

$$\delta E_{\text{o}} = -3306744 \frac{\delta D}{D} E \Lambda_{\text{o}}^2. \quad (\text{D10})$$

Finally, the second order correction to the energy is,

$$\begin{aligned} \delta E = & -\frac{\delta D}{D} E \left\{ \frac{525}{4} \Lambda_{\text{d}}^2 + 13440 \Lambda_{\text{q}}^2 + \right. \\ & \left. + 3306744 \Lambda_{\text{o}}^2 \right\}. \end{aligned} \quad (\text{D11})$$

Appendix E: Derivation of $\delta H_{\beta,\beta',\beta}^{(3)}$, Eq. (35)

We consider $\delta H_{\beta,\beta',\beta}^{(3)}$ for $\beta, \beta' = d, q, o$, in turn.

1. Dipole-dipole contribution: The correction $\delta H_{d,d,d}^{(3)}$ is,

$$\begin{aligned} \delta H_{d,d,d}^{(3)} = & \frac{2\lambda_d^3 \rho_0^2 \delta D}{D} \frac{k_F^3}{a_g^6} \sum_{\alpha_1, \alpha_2, \alpha_3} \sum_{f, f'} \left(\hat{F}^{\alpha_1} \hat{F}^{\alpha_2} \hat{F}^{\alpha_3} \right)_{f, f'} \\ & \times X^{f, f'} \sum_{i, i'} \sum_{n, n'} I_{i, i'}^{\alpha_2} c_{n, i}^\dagger c_{n', i'} \times \\ & \times \text{Tr} \left(\hat{I}^{\alpha_1} \hat{I}^{\alpha_3} \right). \end{aligned} \quad (\text{E1})$$

In order to simplify the expression in the right hand side of eq. (E1), we use the following equalities,

$$\begin{aligned} \text{Tr} \left(\hat{I}^{\alpha_1} \hat{I}^{\alpha_3} \right) &= \frac{1}{3} I(I+1)(2I+1) = \\ &= \frac{35}{2} \delta_{\alpha_1, \alpha_3}, \end{aligned} \quad (\text{E2})$$

$$\begin{aligned} \sum_{\alpha_1} \hat{F}^{\alpha_1} \hat{F}^{\alpha_2} \hat{F}^{\alpha_1} &= \left(F(F+1) - 1 \right) \hat{F}^{\alpha_2} = \\ &= \frac{11}{4} \hat{F}^{\alpha_2}. \end{aligned} \quad (\text{E3})$$

Then the dipole-dipole contribution takes the form,

$$\begin{aligned} \delta H_{d,d,d}^{(3)} = & \frac{385}{4} \frac{\lambda_d^3 \rho_0^2 \delta D}{D} \frac{k_F^3}{a_g^6} \sum_{\alpha} \sum_{f, f'} \sum_{i, i'} \sum_{n, n'} \\ & \times F_{f, f'}^{\alpha} I_{i, i'}^{\alpha} X^{f, f'} c_{n, i}^\dagger c_{n', i'}. \end{aligned} \quad (\text{E4})$$

2. Dipole-quadrupole contribution: The correction $\delta H_{q,d,q}^{(3)}$ is,

$$\begin{aligned} \delta H_{q,d,q}^{(3)} = & \frac{2\lambda_d \lambda_q^2 \rho_0^2 \delta D}{D} \frac{k_F^3}{a_g^6} \sum_{\alpha_1, \alpha'_1} \sum_{\alpha_2} \sum_{\alpha_3, \alpha'_3} \sum_{f, f'} \\ & \times \left(\hat{F}^{\alpha_1, \alpha'_1} \hat{F}^{\alpha_2} \hat{F}^{\alpha_3, \alpha'_3} \right)_{f, f'} \times \\ & \times X^{f, f'} \sum_{i, i'} \sum_{n, n'} I_{i, i'}^{\alpha_2} c_{n, i}^\dagger c_{n', i'} \times \\ & \times \text{Tr} \left(\hat{I}^{\alpha_1, \alpha'_1} \hat{I}^{\alpha_3, \alpha'_3} \right). \end{aligned} \quad (\text{E5})$$

Using eqs. (D6) and (D7), we can write

$$\begin{aligned} \sum_{\alpha_1, \alpha'_1} \sum_{\alpha_3, \alpha'_3} \hat{F}^{\alpha_1, \alpha'_1} \hat{F}^{\alpha_2} \hat{F}^{\alpha_3, \alpha'_3} \text{Tr} \left(\hat{I}^{\alpha_1, \alpha'_1} \hat{I}^{\alpha_3, \alpha'_3} \right) &= \\ &= 1344 \hat{F}^{\alpha_2}. \end{aligned}$$

Then the dipole-quadrupole contribution can be written as,

$$\begin{aligned} \delta H_{q,d,q}^{(3)} = & 2688 \frac{\lambda_d \lambda_q^2 \rho_0^2 \delta D}{D} \frac{k_F^3}{a_g^6} \sum_{\alpha} \sum_{f, f'} \sum_{i, i'} \sum_{n, n'} \\ & \times F_{f, f'}^{\alpha} I_{i, i'}^{\alpha} X^{f, f'} c_{n, i}^\dagger c_{n', i'}. \end{aligned} \quad (\text{E6})$$

3. Dipole-octupole contribution: The correction $\delta H_{o,d,o}^{(3)}$ is,

$$\begin{aligned} \delta H_{o,d,o}^{(3)} = & \frac{2\lambda_d \lambda_o^2 \rho_0^2 \delta D}{D} \frac{k_F^3}{a_g^6} \sum_{\alpha_1, \alpha'_1, \alpha''_1} \sum_{\alpha_2} \sum_{\alpha_3, \alpha'_3, \alpha''_3} \sum_{f, f'} \\ & \times \left(\hat{F}^{\alpha_1, \alpha'_1, \alpha''_1} \hat{F}^{\alpha_2} \hat{F}^{\alpha_3, \alpha'_3, \alpha''_3} \right)_{f, f'} \times \\ & \times X^{f, f'} \sum_{i, i'} \sum_{n, n'} I_{i, i'}^{\alpha_2} c_{n, i}^\dagger c_{n', i'} \times \\ & \times \text{Tr} \left(\hat{I}^{\alpha_1, \alpha'_1, \alpha''_1} \hat{I}^{\alpha_3, \alpha'_3, \alpha''_3} \right). \end{aligned} \quad (\text{E7})$$

Equation (E7) can be simplified by using eq. (D9),

$$\begin{aligned} \sum_{\alpha_1, \alpha'_1, \alpha''_1} \sum_{\alpha_3, \alpha'_3, \alpha''_3} \hat{F}^{\alpha_1, \alpha'_1, \alpha''_1} \hat{F}^{\alpha_2} \hat{F}^{\alpha_3, \alpha'_3, \alpha''_3} \times \\ \times \text{Tr} \left(\hat{I}^{\alpha_1, \alpha'_1, \alpha''_1} \hat{I}^{\alpha_3, \alpha'_3, \alpha''_3} \right) = \\ = - \frac{4960116}{5} \hat{F}^{\alpha_2}. \end{aligned}$$

Then the dipole-quadrupole contribution can be written as,

$$\begin{aligned} \delta H_{o,d,o}^{(3)} = & - \frac{9920232}{5} \frac{\lambda_d \lambda_o^2 \rho_0^2 \delta D}{D} \frac{k_F^3}{a_g^6} \sum_{\alpha} \sum_{f, f'} \sum_{i, i'} \sum_{n, n'} \\ & \times F_{f, f'}^{\alpha} I_{i, i'}^{\alpha} X^{f, f'} c_{n, i}^\dagger c_{n', i'}. \end{aligned} \quad (\text{E8})$$

4. Quadrupole-dipole contribution: The correction $\delta H_{d,q,d}^{(3)}$ is,

$$\begin{aligned} \delta H_{d,q,d}^{(3)} = & \frac{2\lambda_q \lambda_d^2 \rho_0^2 \delta D}{D} \frac{k_F^3}{a_g^6} \sum_{\alpha_1} \sum_{\alpha_2, \alpha'_2} \sum_{\alpha_3} \sum_{f, f'} \\ & \times \left(\hat{F}^{\alpha_1} \hat{F}^{\alpha_2, \alpha'_2} \hat{F}^{\alpha_3} \right)_{f, f'} \times \\ & \times X^{f, f'} \sum_{i, i'} \sum_{n, n'} I_{i, i'}^{\alpha_2, \alpha'_2} c_{n, i}^\dagger c_{n', i'} \times \\ & \times \text{Tr} \left(\hat{I}^{\alpha_1} \hat{I}^{\alpha_3} \right). \end{aligned} \quad (\text{E9})$$

In order to simplify eq. (E9), we use eq. (D3) and the following equality,

$$\sum_{\alpha} \hat{F}^{\alpha} \hat{F}^{\alpha_2, \alpha'_2} \hat{F}^{\alpha} = \frac{3}{4} \hat{F}^{\alpha_2, \alpha'_2}.$$

Then the quadrupole-dipole contribution can be written as,

$$\begin{aligned} \delta H_{d,q,d}^{(3)} = & \frac{105}{4} \frac{\lambda_q \lambda_d^2 \rho_0^2 \delta D}{D} \frac{k_F^3}{a_g^6} \sum_{\alpha} \sum_{f, f'} \sum_{i, i'} \sum_{n, n'} \\ & \times F_{f, f'}^{\alpha} I_{i, i'}^{\alpha} X^{f, f'} c_{n, i}^\dagger c_{n', i'}. \end{aligned} \quad (\text{E10})$$

5. Quadrupole-quadrupole contribution: The correction $\delta H_{q,q,q}^{(3)}$ is,

$$\begin{aligned} \delta H_{q,q,q}^{(3)} = & \frac{2\lambda_q^3 \rho_0^2 \delta D}{D} \frac{k_F^3}{a_g^6} \sum_{\alpha_1, \alpha'_1} \sum_{\alpha_2, \alpha'_2} \sum_{\alpha_3, \alpha'_3} \sum_{f, f'} \\ & \times \left(\hat{F}^{\alpha_1, \alpha'_1} \hat{F}^{\alpha_2, \alpha'_2} \hat{F}^{\alpha_3, \alpha'_3} \right)_{f, f'} \times \\ & \times X^{f, f'} \sum_{i, i'} \sum_{n, n'} I_{i, i'}^{\alpha_2, \alpha'_2} c_{n, i}^\dagger c_{n', i'} \times \\ & \times \text{Tr} \left(\hat{I}^{\alpha_1, \alpha'_1} \hat{I}^{\alpha_3, \alpha'_3} \right). \end{aligned} \quad (\text{E11})$$

Using eqs. (D6) and (D7), we can write

$$\begin{aligned} \sum_{\alpha_1, \alpha'_1} \sum_{\alpha_3, \alpha'_3} \hat{F}^{\alpha_1, \alpha'_1} \hat{F}^{\alpha_2, \alpha'_2} \hat{F}^{\alpha_3, \alpha'_3} \text{Tr} \left(\hat{I}^{\alpha_1, \alpha'_1} \hat{I}^{\alpha_3, \alpha'_3} \right) = \\ = -4032 \hat{F}^{\alpha_2, \alpha'_2}. \end{aligned}$$

Then $\delta H_{q,q,q}^{(3)}$ takes the form,

$$\begin{aligned} \delta H_{q,q,q}^{(3)} = & -8064 \frac{\lambda_q^3 \rho_0^2 \delta D}{D} \frac{k_F^3}{a_g^6} \sum_{\alpha, \alpha'} \sum_{f, f'} \sum_{i, i'} \sum_{n, n'} \\ & \times F_{f, f'}^{\alpha, \alpha'} I_{i, i'}^{\alpha_2, \alpha'_2} X^{f, f'} c_{n, i}^\dagger c_{n', i'}. \end{aligned} \quad (\text{E12})$$

6. Quadrupole-octupole contribution: The correction $\delta H_{o,q,o}^{(3)}$ is,

$$\begin{aligned} \delta H_{o,q,o}^{(3)} = & \frac{2\lambda_q \lambda_o^2 \rho_0^2 \delta D}{D} \frac{k_F^3}{a_g^6} \sum_{\alpha_1, \alpha'_1, \alpha''_1} \sum_{\alpha_2, \alpha'_2, \alpha''_2} \sum_{\alpha_3, \alpha'_3, \alpha''_3} \sum_{f, f'} \\ & \times \left(\hat{F}^{\alpha_1, \alpha'_1, \alpha''_1} \hat{F}^{\alpha_2, \alpha'_2, \alpha''_2} \hat{F}^{\alpha_3, \alpha'_3, \alpha''_3} \right)_{f, f'} \times \\ & \times X^{f, f'} \sum_{i, i'} \sum_{n, n'} I_{i, i'}^{\alpha_2, \alpha'_2} c_{n, i}^\dagger c_{n', i'} \times \\ & \times \text{Tr} \left(\hat{I}^{\alpha_1, \alpha'_1, \alpha''_1} \hat{I}^{\alpha_3, \alpha'_3, \alpha''_3} \right). \end{aligned} \quad (\text{E13})$$

In order to simplify eq. (E13), we use the following equality,

$$\begin{aligned} \sum_{\alpha_1, \alpha'_1, \alpha''_1} \sum_{\alpha_3, \alpha'_3, \alpha''_3} \hat{F}^{\alpha_1, \alpha'_1, \alpha''_1} \hat{F}^{\alpha_2, \alpha'_2, \alpha''_2} \hat{F}^{\alpha_3, \alpha'_3, \alpha''_3} \times \\ \times \text{Tr} \left(\hat{I}^{\alpha_1, \alpha'_1, \alpha''_1} \hat{I}^{\alpha_3, \alpha'_3, \alpha''_3} \right) = \\ = \frac{1153372}{5} \hat{F}^{\alpha_2, \alpha'_2}. \end{aligned}$$

Then eq. (E13) takes the form,

$$\begin{aligned} \delta H_{o,q,o}^{(3)} = & \frac{2306744}{5} \frac{\lambda_q \lambda_o^2 \rho_0^2 \delta D}{D} \frac{k_F^3}{a_g^6} \sum_{\alpha, \alpha'} \sum_{f, f'} \sum_{i, i'} \sum_{n, n'} \\ & \times F_{f, f'}^{\alpha, \alpha'} I_{i, i'}^{\alpha, \alpha'} X^{f, f'} c_{n, i}^\dagger c_{n', i'}. \end{aligned} \quad (\text{E14})$$

7. Octupole-dipole contribution: The correction $\delta H_{d,o,d}^{(3)}$ is,

$$\begin{aligned} \delta H_{d,o,d}^{(3)} = & \frac{2\lambda_o \lambda_d^2 \rho_0^2 \delta D}{D} \frac{k_F^3}{a_g^6} \sum_{\alpha_1} \sum_{\alpha_2, \alpha'_2, \alpha''_2} \sum_{\alpha_3} \sum_{f, f'} \\ & \times \left(\hat{F}^{\alpha_1} \hat{F}^{\alpha_2, \alpha'_2, \alpha''_2} \hat{F}^{\alpha_3} \right)_{f, f'} \times \\ & \times X^{f, f'} \sum_{i, i'} \sum_{n, n'} I_{i, i'}^{\alpha_2, \alpha'_2, \alpha''_2} c_{n, i}^\dagger c_{n', i'} \times \\ & \times \text{Tr} \left(\hat{I}^{\alpha_1} \hat{I}^{\alpha_3} \right). \end{aligned} \quad (\text{E15})$$

In order to simplify eq. (E15), we use the following equality,

$$\begin{aligned} \sum_{\alpha_1, \alpha_3} \hat{F}^{\alpha_1} \hat{F}^{\alpha_2, \alpha'_2, \alpha''_2} \hat{F}^{\alpha_3} \text{Tr} \left(\hat{I}^{\alpha_1} \hat{I}^{\alpha_3} \right) = \\ = -\frac{315}{8} \hat{F}^{\alpha_2, \alpha'_2, \alpha''_2}. \end{aligned}$$

Then the octupole-dipole contribution can be written as,

$$\begin{aligned} \delta H_{d,o,d}^{(3)} = & -\frac{315}{4} \frac{\lambda_o \lambda_d^2 \rho_0^2 \delta D}{D} \frac{k_F^3}{a_g^6} \sum_{\alpha, \alpha', \alpha''} \sum_{f, f'} \sum_{i, i'} \sum_{n, n'} \\ & \times F_{f, f'}^{\alpha, \alpha', \alpha''} I_{i, i'}^{\alpha, \alpha', \alpha''} X^{f, f'} c_{n, i}^\dagger c_{n', i'}. \end{aligned} \quad (\text{E16})$$

8. Octupole-quadrupole contribution: The correction $\delta H_{q,o,q}^{(3)}$ is,

$$\begin{aligned} \delta H_{q,o,q}^{(3)} = & \frac{2\lambda_o \lambda_q^2 \rho_0^2 \delta D}{D} \frac{k_F^3}{a_g^6} \sum_{\alpha_1, \alpha'_1} \sum_{\alpha_2, \alpha'_2, \alpha''_2} \sum_{\alpha_3, \alpha'_3} \sum_{f, f'} \\ & \times \left(\hat{F}^{\alpha_1, \alpha'_1} \hat{F}^{\alpha_2, \alpha'_2, \alpha''_2} \hat{F}^{\alpha_3, \alpha'_3} \right)_{f, f'} \times \\ & \times X^{f, f'} \sum_{i, i'} \sum_{n, n'} I_{i, i'}^{\alpha_2, \alpha'_2, \alpha''_2} c_{n, i}^\dagger c_{n', i'} \times \\ & \times \text{Tr} \left(\hat{I}^{\alpha_1, \alpha'_1} \hat{I}^{\alpha_3, \alpha'_3} \right). \end{aligned} \quad (\text{E17})$$

Using eqs. (D6) and (D7), we can write

$$\begin{aligned} \sum_{\alpha_1, \alpha'_1} \sum_{\alpha_3, \alpha'_3} \hat{F}^{\alpha_1, \alpha'_1} \hat{F}^{\alpha_2, \alpha'_2, \alpha''_2} \hat{F}^{\alpha_3, \alpha'_3} \text{Tr} \left(\hat{I}^{\alpha_1, \alpha'_1} \hat{I}^{\alpha_3, \alpha'_3} \right) = \\ = 1344 \hat{F}^{\alpha_2, \alpha'_2, \alpha''_2}. \end{aligned}$$

Then $\delta H_{q,o,q}^{(3)}$ takes the form,

$$\begin{aligned} \delta H_{q,o,q}^{(3)} = & 2688 \frac{\lambda_o \lambda_q^2 \rho_0^2 \delta D}{D} \frac{k_F^3}{a_g^6} \sum_{\alpha, \alpha', \alpha''} \sum_{f, f'} \sum_{i, i'} \sum_{n, n'} \\ & \times F_{f, f'}^{\alpha, \alpha', \alpha''} I_{i, i'}^{\alpha, \alpha', \alpha''} X^{f, f'} c_{n, i}^\dagger c_{n', i'}. \end{aligned} \quad (\text{E18})$$

9. Octuple-octuple contribution: The correction $\delta H_{\text{o,o,o}}^{(3)}$ is,

$$\begin{aligned} \delta H_{\text{o,o,o}}^{(3)} = & \frac{2\lambda_{\text{o}}^3 \rho_0^2 \delta D}{D} \frac{k_F^3}{a_{\text{g}}^6} \sum_{\alpha_1, \alpha'_1, \alpha''_1} \sum_{\alpha_2, \alpha'_2, \alpha''_2} \sum_{\alpha_3, \alpha'_3, \alpha''_3} \sum_{f, f'} \\ & \times \left(\hat{F}^{\alpha_1, \alpha'_1, \alpha''_1} \hat{F}^{\alpha_2, \alpha'_2, \alpha''_2} \hat{F}^{\alpha_3, \alpha'_3, \alpha''_3} \right)_{f, f'} \times \\ & \times X^{f, f'} \sum_{i, i'} \sum_{n, n'} I_{i, i'}^{\alpha_2, \alpha'_2, \alpha''_2} c_{n, i}^\dagger c_{n', i'} \times \\ & \times \text{Tr} \left(\hat{I}^{\alpha_1, \alpha'_1, \alpha''_1} \hat{I}^{\alpha_3, \alpha'_3, \alpha''_3} \right). \end{aligned} \quad (\text{E19})$$

In order to simplify eq. (E19), we use the following equality,

$$\begin{aligned} & \sum_{\alpha_1, \alpha'_1, \alpha''_1} \sum_{\alpha_3, \alpha'_3, \alpha''_3} \hat{F}^{\alpha_1, \alpha'_1, \alpha''_1} \hat{F}^{\alpha_2, \alpha'_2, \alpha''_2} \hat{F}^{\alpha_3, \alpha'_3, \alpha''_3} \times \\ & \times \text{Tr} \left(\hat{I}^{\alpha_1, \alpha'_1, \alpha''_1} \hat{I}^{\alpha_3, \alpha'_3, \alpha''_3} \right) = \\ & = -\frac{236196}{5} \hat{F}^{\alpha_2, \alpha'_2, \alpha''_2}. \end{aligned}$$

Then eq. (E19) takes the form,

$$\begin{aligned} \delta H_{\text{o,o,o}}^{(3)} = & -\frac{472392}{5} \frac{\lambda_{\text{o}}^3 \rho_0^2 \delta D}{D} \frac{k_F^3}{a_{\text{g}}^6} \sum_{\alpha, \alpha', \alpha''} \sum_{f, f'} \sum_{i, i'} \sum_{n, n'} \\ & \times F_{f, f'}^{\alpha, \alpha', \alpha''} I_{i, i'}^{\alpha, \alpha', \alpha''} X^{f, f'} c_{n, i}^\dagger c_{n', i'}. \end{aligned} \quad (\text{E20})$$

Appendix F: Eigenfunctions and Eigenenergy of the Dipole-Dipole, Quadrupole-Quadrupole and Octupole-Octupole Interactions

Appendix F main points The dipole-dipole, quadrupole-quadrupole and octopod-octopod Hamiltonians are defined in Eqs. (F1, F5, F8) respectively. Their eigenfunctions and eigenenergies, required for the calculations of the exchange constants, are explicitly elucidated in this Appendix.

Consider four atoms, such that one atom (an “impurity atom”) has spin $F = \frac{3}{2}$ and the three other atoms (“itinerant atoms”) have spin $I = \frac{5}{2}$. The interaction between the itinerant atoms and the impurity is dipole-dipole, quadrupole-quadrupole and octupole-octupole interactions. We derive here eigenfunctions and corresponding eigenenergies of the Hamiltonians of the dipole-dipole, quadrupole-quadrupole and octupole-octupole interactions, in turn.

1. Eigenfunctions of the Dipole-Dipole Interaction

The Hamiltonian of the dipole-dipole interaction between the atoms is,

$$\mathcal{H}_{\text{d}} = \lambda_{\text{d}} \left(\hat{\mathbf{F}} \cdot \hat{\mathbf{S}} \right), \quad (\text{F1})$$

where $\hat{\mathbf{F}}$ is a vector of the spin- $\frac{3}{2}$ operators, $\hat{\mathbf{S}} = \hat{\mathbf{I}}_1 + \hat{\mathbf{I}}_2 + \hat{\mathbf{I}}_3$, where $\hat{\mathbf{I}}_a$ ($a = 1, 2, 3$) is a vector of the spin- $\frac{5}{2}$ operators.

Note that \mathcal{H}_{d} can be expressed in terms of the two-atomic spin $\hat{\mathbf{L}}$,

$$\mathcal{H}_{\text{d}} = \frac{\lambda_{\text{d}}}{2} \left(\hat{\mathbf{L}}^2 - F(F+1) - S(S+1) \right), \quad (\text{F2})$$

where

$$\hat{\mathbf{L}} = \hat{\mathbf{F}} + \hat{\mathbf{S}},$$

Eq. (F2) shows that \mathcal{H}_{d} commutes with $\hat{\mathbf{L}}^2$, $\hat{\mathbf{F}}^2$ and $\hat{\mathbf{F}}^2$. In addition, \mathcal{H}_{d} commutes with $\hat{\mathbf{L}}^z$, but neither with $\hat{\mathbf{F}}^z$ nor $\hat{\mathbf{I}}^z$. The eigenfunctions of \mathcal{H}_{d} , $|L, L_z\rangle$, are defined as

$$\begin{aligned} \hat{\mathbf{L}}^2 |L, L_z\rangle &= L(L+1) |L, L_z\rangle, \\ \hat{\mathbf{L}}^z |L, L_z\rangle &= L_z |L, L_z\rangle, \end{aligned}$$

where $L = 1, 2, 3, 4$. The corresponding eigenvalues of \mathcal{H}_{d} are,

$$\mathcal{E}_L^{(\text{d})} = \lambda_{\text{d}} \mathcal{D}_L, \quad (\text{F3})$$

where

$$\mathcal{D}_L = \frac{1}{2} \left(L(L+1) - F(F+1) - S(S+1) \right). \quad (\text{F4})$$

When $\lambda_{\text{d}} > 0$, the lowest energy level has maximal value of S and minimal value of L . For $I = \frac{5}{2}$, this is the level $S = \frac{9}{2}$ and $L = 3$ (see discussions in Sec. IX). Therefore, we conclude that the interaction is antiferromagnetic.

2. Eigenfunctions of the Quadrupole-Quadrupole Interaction

The Hamiltonian of the quadrupole-quadrupole interaction between the atoms is,

$$\mathcal{H}_{\text{q}} = \lambda_{\text{q}} \sum_{\alpha, \alpha'} \hat{F}^{\alpha, \alpha'} \hat{S}^{\alpha, \alpha'}, \quad (\text{F5})$$

where $\hat{F}^{\alpha, \alpha'}$ or $\hat{S}^{\alpha, \alpha'}$ is a quadrupole operator for the atom with spin- $\frac{3}{2}$ or spin- $\frac{9}{2}$,

$$\begin{aligned} \hat{F}^{\alpha, \alpha'} &= \hat{F}^\alpha \hat{F}^{\alpha'} + \hat{F}^{\alpha'} \hat{F}^\alpha - \frac{2}{3} F(F+1) \delta_{\alpha, \alpha'}, \\ \hat{S}^{\alpha, \alpha'} &= \hat{S}^\alpha \hat{S}^{\alpha'} + \hat{S}^{\alpha'} \hat{S}^\alpha - \frac{2}{3} S(S+1) \delta_{\alpha, \alpha'}. \end{aligned}$$

\mathcal{H}_{q} can be expressed in terms of $(\hat{\mathbf{F}} \cdot \hat{\mathbf{S}})$ as,

$$\begin{aligned} \mathcal{H}_{\text{q}} = & \lambda_{\text{q}} \left\{ 4 (\hat{\mathbf{F}} \cdot \hat{\mathbf{S}})^2 + 2 (\hat{\mathbf{F}} \cdot \hat{\mathbf{S}}) - \right. \\ & \left. - \frac{4}{3} F(F+1) S(S+1) \right\}. \end{aligned}$$

Eigenfunctions of \mathcal{H}_{q} are $|L, L_z\rangle$. Corresponding eigenenergies are,

$$\mathcal{E}_L^{(\text{q})} = \lambda_{\text{q}} \mathcal{Q}_L, \quad (\text{F6})$$

where

$$\mathcal{Q}_L = 4 \mathcal{D}_L^2 + 2 \mathcal{D}_L - \frac{4}{3} F(F+1) S(S+1),$$

\mathcal{D}_L is given by eq. (F4).

The spin L takes the values $L = 3, 4, 5, 6$. Corresponding energies are,

$$\begin{aligned} \mathcal{E}_3^{(q)} &= 132 \lambda_q, \\ \mathcal{E}_4^{(q)} &= -60 \lambda_q, \\ \mathcal{E}_5^{(q)} &= -120 \lambda_q, \\ \mathcal{E}_6^{(q)} &= 72 \lambda_q. \end{aligned} \quad (\text{F7})$$

It is seen that when $\lambda_q < 0$, the lowest energy level is the $L = 1$ energy level. For $\lambda_q > 0$, the lowest energy level is the $L = 5$ energy level.

3. Eigenfunctions of the Octuple-Octuple Interaction

The Hamiltonian of the octuple-octuple interaction between the impurity and the itinerant atoms is,

$$\mathcal{H}_o = \lambda_o \sum_{\alpha, \alpha', \alpha''} \hat{F}^{\alpha, \alpha', \alpha''} \hat{S}^{\alpha, \alpha', \alpha''}, \quad (\text{F8})$$

where $\hat{F}^{\alpha, \alpha', \alpha''}$ or $\hat{S}^{\alpha, \alpha', \alpha''}$ is an octuple operator for the atom with spin- $\frac{3}{2}$ or spin- $\frac{9}{2}$, see eq. (5).

Substituting eq. (5) into eq. (F8), we get

$$\begin{aligned} \mathcal{H}_o = \lambda_o \left\{ & 36 (\hat{\mathbf{F}} \cdot \hat{\mathbf{I}})^3 + 72 (\hat{\mathbf{F}} \cdot \hat{\mathbf{I}})^2 + 12 (\hat{\mathbf{F}} \cdot \hat{\mathbf{I}}) - \right. \\ & - \frac{12}{5} (3F(F+1) - 1)(3S(S+1) - 1)(\hat{\mathbf{F}} \cdot \hat{\mathbf{I}}) - \\ & \left. - 18 F(F+1) S(S+1) \right\}. \end{aligned}$$

The spin L takes the values $L = 3, 4, 5, 6$. Corresponding energies are,

$$\begin{aligned} \mathcal{E}_3^{(o)} &= -\frac{11088}{5} \lambda_o, \\ \mathcal{E}_4^{(o)} &= \frac{22368}{5} \lambda_o, \\ \mathcal{E}_5^{(o)} &= -\frac{14787}{5} \lambda_o, \\ \mathcal{E}_6^{(o)} &= 2997 \lambda_o. \end{aligned} \quad (\text{F9})$$

It is seen that when $\lambda_o < 0$, the lowest energy level is the $L = 4$ energy level. When $\lambda_o > 0$, the lowest energy level is the $L = 5$ energy level.

Screening of the impurity spin by a cloud of itinerant atoms is illustrated in Fig. 13. Here the red disk denotes the impurity atom with spin F , the blue disk denotes a cloud of itinerant atoms with the total spin S . The green arrow is a “dressed” spin of the impurity $\mathbf{L} = \mathbf{F} + \mathbf{S}$. When the lowest energy state is $|3, L_z\rangle$ or $|4, L_z\rangle$, the “dressed” spin of the impurity \mathbf{L} is antiparallel to the “bare” spin \mathbf{F} [see inequality (52)], and therefore we deal with over-screened KE.

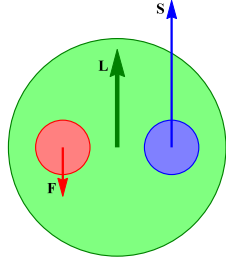


FIG. 13: (color online) Impurity atom with spin F (red disk), itinerant atoms with total spin S (blue disk) creating a cloud screening the spin of the impurity. The spin of the “dressed” impurity is L .

Appendix G: Yb(3P_2) Atom in Magnetic Field

Appendices G and H main points: Although we do not subject our system to an external magnetic field (since it is detrimental for the KE) we find it useful to employ our detailed analysis of Yb atoms and inspect their properties under an application of a weak magnetic field. In particular, the multiple analysis worked out in this paper helps us to elucidate the pattern of the dependence of energy levels on the magnetic field, both for the ground-state 1S_0 and the excited state 3P_2 . This is shown in Figs. 14(a), and 14(b).

Consider an 3P_2 Yb atom in external magnetic field. The Hamiltonian of the atom is,

$$\mathcal{H}_{\text{at}} = \mathcal{H}_{\text{at}}^{(0)} + \mathcal{H}_B, \quad (\text{G1})$$

where $\mathcal{H}_{\text{at}}^{(0)}$ is a Hamiltonian of the isolated ^{173}Yb atom in the 3P_2 state and \mathcal{H}_B describes interaction of the atom with the magnetic field,

$$\mathcal{H}_{\text{at}}^{(0)} = A_d \sum_{\alpha} \hat{I}^{\alpha} \hat{J}^{\alpha} + A_q \sum_{\alpha, \alpha'} \hat{I}^{\alpha, \alpha'} \hat{J}^{\alpha, \alpha'}, \quad (\text{G2})$$

$$\mathcal{H}_B = -g\mu_B B \hat{J}^z. \quad (\text{G3})$$

Here \hat{I}^{α} and $\hat{I}^{\alpha, \alpha'}$ are spin and quadrupole angular momentum operators for the nucleus, whereas J^{α} and $J^{\alpha, \alpha'}$ are orbital angular momentum and quadrupole angular momentum operators of the 3P_2 electronic configuration. g is the electronic g-factor of the Yb atom in the 3P_2 state, see eq. (67).

The constants A_d and A_q are³⁴,

$$\frac{A_d}{h} = -738 \text{ MHz}, \quad \frac{A_q}{h} = 1312 \text{ MHz}, \quad (\text{G4})$$

where h is the Planck constant, or

$$A_d = -3.052 \text{ } \mu\text{eV}, \quad A_q = 5.426 \text{ } \mu\text{eV}.$$

Taking into account definition (3) for the quadrupole angular momentum operators, we can write the Hamiltonian (G2) in the form,

$$\begin{aligned} \mathcal{H}_{\text{at}}^{(0)} = & (A_d - 2 A_q) (\hat{\mathbf{I}} \cdot \hat{\mathbf{J}}) + 4 A_q (\hat{\mathbf{I}} \cdot \hat{\mathbf{J}})^2 - \\ & - \frac{4}{3} A_q I(I+1) J(J+1). \end{aligned} \quad (\text{G5})$$

Eq. (G5) shows that eigenfunctions of $\mathcal{H}_{\text{at}}^{(0)}$ are also eigenfunctions of the operators $\hat{\mathbf{F}}^2$ and \hat{F}^z [where $\hat{\mathbf{F}} = \hat{\mathbf{I}} + \hat{\mathbf{J}}$ is the operator of the total atomic orbital momentum],

$$|F, f\rangle = \sum_{i,j} C_{I,i;J,j}^{F,f} |I, i; J, j\rangle, \quad (\text{G6})$$

where i, j and f are nuclear, electronic and total atomic magnetic quantum numbers. The wave functions $|I, i; J, j\rangle$ as eigenfunctions of the operators \hat{I}^z and \hat{J}^z ,

$$\begin{aligned} \hat{I}^z |I, i; J, j\rangle &= i |I, i; J, j\rangle, \\ \hat{J}^z |I, i; J, j\rangle &= j |I, i; J, j\rangle. \end{aligned}$$

Corresponding eigenenergies $\mathcal{E}_L^{(0)}$ are

$$\begin{aligned} \mathcal{E}_{\frac{1}{2}}^{(0)} &= -7A_d + 140A_q = 781.0 \text{ } \mu\text{eV}, \\ \mathcal{E}_{\frac{3}{2}}^{(0)} &= -\frac{11}{2} A_d + 62A_q = 353.2 \text{ } \mu\text{eV}, \\ \mathcal{E}_{\frac{5}{2}}^{(0)} &= -3A_d - 28A_q = -142.8 \text{ } \mu\text{eV}, \\ \mathcal{E}_{\frac{7}{2}}^{(0)} &= \frac{1}{2} A_d - 70 A_q = -381.3 \text{ } \mu\text{eV}, \\ \mathcal{E}_{\frac{9}{2}}^{(0)} &= 5 A_d + 20 A_q = 93.2 \text{ } \mu\text{eV}. \end{aligned}$$

The interaction Hamiltonian \mathcal{H}_B , eq. (G3), commutes with the operator \hat{F}^z , but not with $\hat{\mathbf{F}}^2$. Therefore, eigenfunctions of the Hamiltonian \mathcal{H}_{at} , eq. (G1), are described by the magnetic quantum numbers f , but not by the total atomic spin F .

In order to find eigenenergies of the Hamiltonian (G1), we find the matrix elements of \mathcal{H}_B ,

$$\begin{aligned} V_{F,F'}^{(f)} &= \langle F, f | \mathcal{H}_B | F', f \rangle = \\ &= -g\mu_B B \mathcal{C}_{F,F'}^{(f)}, \end{aligned} \quad (\text{G7})$$

where

$$\mathcal{C}_{F,F'}^{(f)} = \sum_{i,j} j C_{I,i;J,j}^{F,f} C_{I,i;J,j}^{F',f},$$

where $f = -\frac{9}{2}, -\frac{7}{2}, \dots, \frac{9}{2}$ and $f \leq F, F' \leq \frac{9}{2}$. Then the eigenenergies of $\hat{\mathcal{H}}_{\text{at}}$ are found from diagonalization of the matrices $\hat{h}^{(f)}$ with matrix elements $h_{F,F'}^{(f)}$ given by,

$$h_{F,F'}^{(f)} = \mathcal{E}_F^{(0)} \delta_{F,F'} + V_{F,F'}^{(f)}. \quad (\text{G8})$$

The eigenvalues of the Hamiltonian (G1) as functions of the magnetic field are shown in Fig. 14(a). It is seen that for weak magnetic field [when $g\mu_B B$ is small with respect to the hyperfine splitting], every energy level $\mathcal{E}_F^{(0)}$ splits into $2F + 1$ spectral lines with energies $\mathcal{E}_{F,f}$ given by

$$\mathcal{E}_{F,f} = \mathcal{E}_F^{(0)} - g\mu_B B \mathcal{C}_{F,F'}^{(f)}. \quad (\text{G9})$$

For strong magnetic field [when $g\mu_B B$ is large with respect to the hyperfine splitting], the ${}^3\text{P}_2$ energy level

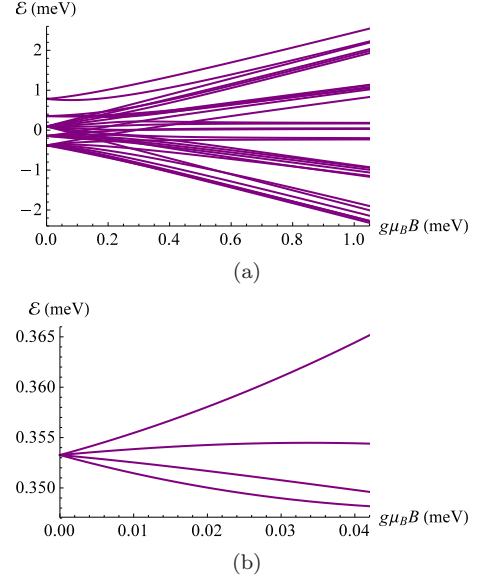


FIG. 14: (color online) Energy spectrum of the ${}^{173}\text{Yb}$ atom in the ${}^3\text{P}_2$ quantum state [panel (a)]. Zeeman splitting of the $F = \frac{3}{2}$ energy level by a weak magnetic field [panel (b)].

splits into 5 levels with $j_z = 0, \pm 1, \pm 2$, and every level splits into six levels by the hyperfine interaction.

Splitting of the $F = \frac{3}{2}$ energy level (that we are interested in) is,

$$\mathcal{E}_{\frac{3}{2},f} = \mathcal{E}_F^{(0)} - \frac{13}{30} g\mu_B B - f g\mu_B B. \quad (\text{G10})$$

Energies $\mathcal{E}_{\frac{3}{2},f}$ calculated numerically by diagonalization of the matrices (G8) are shown in Fig. 14(b) as functions of the magnetic field. The energies are almost linear with the magnetic field which agrees with equation (G10).

Appendix H: Averaged Dipole, Quadrupole and Octupole Moments

The density matrix of the impurity atom placed in the magnetic field $\mathbf{B} = B\mathbf{e}_z$ is,

$$\hat{\rho}_i = \frac{1}{Z_i} \sum_f e^{\beta g\mu_B B f} X^{f,f}, \quad (\text{H1})$$

where $\beta = \frac{1}{T}$,

$$Z_i = \sum_f e^{\beta g\mu_B B f}.$$

Expectation value of an operator $\hat{\mathcal{O}}$ acting in the Hilbert state of quantum states of the isolated impurity is,

$$\langle \hat{\mathcal{O}} \rangle = \frac{1}{Z_i} \sum_f \mathcal{O}_{f,f},$$

where $\mathcal{O}_{f,f} = \langle f | \hat{O} | f \rangle$.

1. Expectation value of the magnetic dipole angular momentum operator is,

$$\langle \hat{F}^\alpha \rangle = -\mathcal{F}_d \delta^{\alpha,z}, \quad (\text{H2})$$

where

$$\mathcal{F}_d = \frac{1}{2} \tanh\left(\frac{g\mu_B B}{2T}\right) + \tanh\left(\frac{g\mu_B B}{T}\right).$$

When $g\mu_B B \ll T$, \mathcal{F}_d can be written in the linear with B approximation as,

$$\mathcal{F}_d = \frac{5}{4} \frac{g\mu_B B}{T} + O\left(\frac{\mu_B^3 B^3}{T^3}\right).$$

2. Expectation value of the magnetic quadrupole angular momentum operator is,

$$\langle \hat{F}^{\alpha,\alpha'} \rangle = -\mathcal{F}_q \delta^{\alpha,\alpha'} \left\{ \delta^{\alpha,x} + \delta^{\alpha,y} - 2\delta^{\alpha,z} \right\}, \quad (\text{H3})$$

where

$$\mathcal{F}_q = \frac{2 \sinh^2\left(\frac{g\mu_B B}{2T}\right)}{\cosh\left(\frac{g\mu_B B}{2T}\right)}.$$

When $g\mu_B B \ll T$, \mathcal{F}_q can be expanded with B as,

$$\mathcal{F}_q = \frac{1}{2} \frac{(g\mu_B B)^2}{T^2} + O\left(\frac{\mu_B^4 B^4}{T^4}\right).$$

3. Expectation value of the magnetic octupole angular momentum operator is,

$$\langle \hat{F}^{\alpha,\alpha',\alpha''} \rangle = \mathcal{F}_o \left\{ \delta^{\alpha,\alpha'} \delta^{\alpha'',z} + \delta^{\alpha,\alpha''} \delta^{\alpha',z} + \delta^{\alpha',\alpha''} \delta^{\alpha,z} - 5 \delta^{\alpha,z} \delta^{\alpha',z} \delta^{\alpha'',z} \right\}, \quad (\text{H4})$$

where

$$\mathcal{F}_o = \frac{36}{5} \frac{2 \sinh^4\left(\frac{g\mu_B B}{2T}\right)}{\sinh\left(\frac{2g\mu_B B}{2T}\right)}.$$

When $g\mu_B B \ll T$, \mathcal{F}_o can be expanded with B as,

$$\mathcal{F}_o = \frac{9}{40} \frac{(g\mu_B B)^3}{T^3} + O\left(\frac{\mu_B^5 B^5}{T^4}\right).$$

4. Expectation value of $F^{\alpha_1} F^{\alpha_2}$ is,

$$\frac{1}{2} \langle \hat{F}^{\alpha_1} \hat{F}^{\alpha_2} + \hat{F}^{\alpha_2} \hat{F}^{\alpha_1} \rangle = \left(\frac{5}{4} + \mathcal{F}_{d,d}^{\alpha_1} \right) \delta^{\alpha_1,\alpha_2}, \quad (\text{H5})$$

where

$$\mathcal{F}_{d,d}^{\alpha} = \left(3 \delta^{\alpha,z} - 1 \right) \frac{2 \sinh^2\left(\frac{g\mu_B B}{2T}\right)}{\cosh\left(\frac{g\mu_B B}{2T}\right)}.$$

When $g\mu_B B \ll T$, $\mathcal{F}_{d,d}$ can be expanded with B as,

$$\mathcal{F}_{d,d}^{\alpha} = \left(3 \delta^{\alpha,z} - 1 \right) \frac{1}{2} \frac{(g\mu_B B)^2}{T^2} + O\left(\frac{\mu_B^4 B^4}{T^4}\right).$$

5. Expectation value of $F^{\alpha_1} F^{\alpha_2, \alpha'_2}$ is,

$$\begin{aligned} \frac{1}{2} \langle \hat{F}^{\alpha_1} \hat{F}^{\alpha_2, \alpha'_2} + \hat{F}^{\alpha_2, \alpha'_2} \hat{F}^{\alpha_1} \rangle &= \\ &= \left(\delta^{\alpha_1,\alpha_2} \delta^{\alpha'_2,z} + \delta^{\alpha_1,\alpha'_2} \delta^{\alpha_2,z} - \right. \\ &\quad \left. - 2 \delta^{\alpha_1,z} \delta^{\alpha_2,z} \delta^{\alpha'_2,z} \right) \mathcal{F}_{d,q}^{(1)} + \\ &\quad + \delta^{\alpha_2,\alpha'_2} \left(\delta^{\alpha_1,z} - 2 \delta^{\alpha_1,z} \delta^{\alpha_2,z} \right) \mathcal{F}_{d,q}^{(2)}, \quad (\text{H6}) \end{aligned}$$

where

$$\mathcal{F}_{d,q}^{(1)} = -\frac{3}{2} \tanh\left(\frac{g\mu_B B}{T}\right),$$

$$\mathcal{F}_{d,q}^{(2)} = \tanh\left(\frac{g\mu_B B}{2T}\right) - \frac{1}{2} \tanh\left(\frac{g\mu_B B}{T}\right).$$

When $g\mu_B B \ll T$, $\mathcal{F}_{d,q}^{(1,2)}$ can be expanded with B as,

$$\begin{aligned} \mathcal{F}_{d,q}^{(1)} &= -\frac{3}{2} \frac{g\mu_B B}{T} + O\left(\frac{\mu_B^3 B^3}{T^3}\right), \\ \mathcal{F}_{d,q}^{(2)} &= \frac{g\mu_B B}{T} + O\left(\frac{\mu_B^3 B^3}{T^3}\right). \end{aligned}$$

6. Expectation value of $F^{\alpha_1} F^{\alpha_2, \alpha'_2, \alpha''_2}$ is,

$$\begin{aligned} \frac{1}{2} \langle \hat{F}^{\alpha_1} \hat{F}^{\alpha_2, \alpha'_2, \alpha''_2} + \hat{F}^{\alpha_2, \alpha'_2, \alpha''_2} \hat{F}^{\alpha_1} \rangle &= \\ &= \mathcal{A}^{\alpha_1; \alpha_2, \alpha'_2, \alpha''_2} \mathcal{F}_{d,o}, \quad (\text{H7}) \end{aligned}$$

where $\mathcal{A}^{\alpha_1; \alpha_2, \alpha'_2, \alpha''_2}$ is symmetric with $\alpha_2, \alpha'_2, \alpha''_2$ tensor which does not depend on temperature or magnetic field,

$$\mathcal{F}_{d,o} = \frac{2 \sinh^2\left(\frac{g\mu_B B}{2T}\right)}{\cosh\left(\frac{g\mu_B B}{2T}\right)}.$$

When $g\mu_B B \ll T$, $\mathcal{F}_{d,o}$ can be expanded with B as,

$$\mathcal{F}_{d,o} = \frac{1}{2} \frac{(g\mu_B B)^2}{T^2} + O\left(\frac{\mu_B^4 B^4}{T^4}\right).$$

¹ J.Kondo, Progr. Theor. Phys. **32**, 37 (1964).

² P. Coleman, Physics World **12**, 29 (1995).

³ P. W. Anderson, Physics World **12**, 37 (1995).

⁴ A. C. Hewson, The Kondo Problem to Heavy Fermions (Cambridge University Press, Cambridge, 1993).

⁵ V. T. Rajan, Phys. Rev. Lett. **51**, 308 (1983).

⁶ P. Schlottmann, Zeitschrift für Physik B: Condensed Matter **51**, 223 (1983).

⁷ Andrés Jerez, Natan Andrei, and Gergely Zaránd, Phys. Rev. B **58**, 3814 (1998).

⁸ P. Nozières and A. Blandin, J. Phys. (Paris) **41**, 193 (1980).

⁹ Y. Oreg and D. Goldhaber-Gordon, Phys. Rev. Lett. **90**, 136602 (2003).

¹⁰ A. M. Sengupta and Y. B. Kim, Phys. Rev. B **54**, 14918 (1996).

¹¹ C. Silber, S. Gunther, C. Marzok, B. Deh, P. W. Courteille, and C. Zimmermann, Phys. Rev. Lett. **95**, 170408 (2005).

¹² T. Onimaru, K. Izawa, K. T. Matsumoto, T. Yoshida, Y. Machida, T. Ikeura, K. Wakiya, K. Umeo, S. Kittaka, K. Araki, T. Sakakibara, T. Takabatake, Phys. Rev. B **94**, 075134 (2016); arXiv:1606.09571.

¹³ I. Kuzmenko, T. Kuzmenko, Y. Avishai and K. A. Kikoin, Phys. Rev. B **91**, 165131 (2015); arXiv:1402.0187.

¹⁴ Olivier Parcollet, Antoine Georges, Gabriel Kotliar, and Anirvan Sengupta, Phys. Rev. B **58**, 3794 (1998); arXiv:cond-mat/9711192.

¹⁵ T. Fukuhara, Y. Takasu, M. Kumakura, Y. Takahashi, Phys. Rev. Lett. **98**, 030401 (2007).

¹⁶ Ren Zhang, Yanting Cheng, Hui Zhai, Peng Zhang, Phys. Rev. Lett. **115**, 135301 (2015); arXiv:1504.02864.

¹⁷ Luis Rieger, Nelson Darkwah Oppong, Moritz Höfer, Diogo Rio Fernandes, Immanuel Bloch, Simon Fölling, arXiv:1708.03810 (2017)

¹⁸ Ren Zhang, Deping Zhang, Yanting Cheng, Wei Chen, Peng Zhang, Hui Zhai, Phys. Rev. A **93**, 043601 (2016); arXiv:1509.01350.

¹⁹ G. Pagano, M. Mancini, G. Cappellini, L. Livi, C. Sias, J. Catani, M. Inguscio, and L. Fallani, Phys. Rev. Lett. **115**, 265301 (2015).

²⁰ Guido Pagano, Marco Mancini, Giacomo Cappellini, Pietro Lombardi, Florian Schäfer, Hui Hu, Xia-Ji Liu, Jacopo Catani, Carlo Sias, Massimo Inguscio and Leonardo Fallani, Nature Physics **10**, 198 (2014).

²¹ Giacomo Cappellini, Marco Mancini, Guido Pagano, Pietro Lombardi, Lorenzo Livi, Mario Siciliani de Cumis, Pablo Cancio, Marco Pizzocaro, Davide Calonico, Filippo Levi, Carlo Sias, Jacopo Catani, Massimo Inguscio, Leonardo Fallani, Phys. Rev. Lett. **113**, 120402 (2014).

²² F. Scazza, C. Hofrichter, M. Höfer, P. C. De Groot, I. Bloch, and S. Fölling, Nature Physics **10**, 779 (2014).

²³ T. D. Ladd, F. Jelezko, R. Laflamme, Y. Nakamura, C. Monroe, and J. L. O'Brien, Nature **464**, 45 (2010).

²⁴ A. J. Daley, Quantum Information Processing **10**, 865 (2011).

²⁵ X. Zhang, M. Bishop, S. L. Bromley, C. V. Kraus, M. S. Safronova, P. Zoller, A. M. Rey, and J. Ye, Science **345**, 1467 (2014).

²⁶ B. Song, C. He, S. Zhang, E. Hajiyev, W. Huang, X.-J. Liu, and G.-B. Jo, Physical Review A Rapid Communications **94**, 061604(R) (2016).

²⁷ S. Kolkowitz, S. L. Bromley, T. Bothwell, M. L. Wall, G. E. Marti, A. P. Koller, X. Zhang, A. M. Rey, and J. Ye, Nature **542**, 6670 (2017).

²⁸ L. F. Livi, G. Cappellini, M. Diem, L. Franchi, C. Clivati, M. Frittelli, F. Levi, D. Calonico, J. Catani, M. Inguscio, L. Fallani, arXiv:1609.04800.

²⁹ Bo Song, Long Zhang, Chengdong He, Ting Fung Jeffrey Poon, Elnur Hajiyev, Shanchao Zhang, Xiong-Jun Liu and Gyu-Boong Jo, arXiv:1706.00768 (2017).

³⁰ S.L. Bromley, S. Kolkowitz, T. Bothwell, D. Kedar, A. Safavi-Naini, M.L. Wall, C. Salomon, A.M. Rey, J. Ye, arXiv:1708.02704 (2017).

³¹ Igor Kuzmenko, Tetyana Kuzmenko, Yshai Avishai, Gyu-Boong Jo, Phys. Rev. B **93**, 115143 (2016); arXiv:1512.00978.

³² A. Yamaguchi, S. Uetake, S. Kato, H. Ito, and Y. Takahashi, New Journal of Physics **12**, 103001 (2010).

³³ A. Khramov, A. Hansen, W. Dowd, R. J. Roy, C. Makrides, A. Petrov, S. Kotochigova, and S. Gupta, Physical Rev. Lett. **112**, 033201 (2014).

³⁴ S.G. Porsev, Yu.G. Rakhlina, M.G. Kozlov, J. Phys. B **32**, 1113-20 (1999); arXiv:physics/9810011.

³⁵ Masses, nuclear spins, and magnetic moments: I. Mills, T. Cvitas, K. Homann, N. Kallay, and K. Kuchitsu, in Quantities, Units and Symbols in Physical Chemistry, Blackwell Scientific Publications, Oxford, UK, 1988.

³⁶ S.G. Porsev, M.S. Safronova, A. Derevianko, Charles W. Clark, Phys. Rev. A **89**, 012711 (2014); arXiv:1307.2656.

³⁷ W. F. Meggers and J. L. Tech, J. Res. Natl. Bur. Stand. (U.S.) **83**, 13 (1978).

³⁸ T. Andersen, "Atomic negative ions: Structure, dynamics and collisions". Physics Reports **394**, 157 (2004).

³⁹ G. F. Gribakin and V. V. Flambaum, Phys. Rev. A **48**, 546 (1993).

⁴⁰ Masaaki Kitagawa, Katsunari Enomoto, Kentaro Kasa, Yoshiro Takahashi, Roman Ciurylo, Pascal Naidon, and Paul S. Julienne, Phys. Rev. A **77**, 012719 (2008); arXiv:0708.0752.

⁴¹ Shinya Kato, Seiji Sugawa, Kosuke Shibata, Ryuta Yamamoto, and Yoshiro Takahashi, Phys. Rev. Lett. **110**, 173201 (2013); arXiv:1210.2483.

⁴² L. D. Landau and E. M. Lifshitz, Quantum Mechanics, A Course of Theoretical Physics Vol. 3 (Pergamon, New York, 1965).

⁴³ Nir Navon, Swann Piatecki, Kenneth Günter, Benno Rem, Trong Canh Nguyen, Frédéric Chevy, Werner Krauth, and Christophe Salomon, Phys. Rev. Lett. **107**, 135301 (2011).

⁴⁴ Nascimbène, S and Navon, N and Jiang, K J and Chevy, F. and SALOMON, C, Nature **463**, 1057 (2010)

⁴⁵ Hofrichter, Christian and Rieger, Luis and Scazza, Francesco and Höfer, Moritz and Fernandes, Diogo Rio and Bloch, Immanuel and Fölling, Simon, Physical Review X, **6**, 021030 (2016)

⁴⁶ Qi Zhou and T.-L. Ho, Nature Physics, **6**(2), 131 (2009)

⁴⁷ G. Valtolina, F. Scazza, A. Amico, A. Burchianti, A. Recati, T. Enss, M. Inguscio, M. Zaccanti, G. Roati, arXiv:1605.07850 (2016)

⁴⁸ Sanner, Christian and Su, Edward J and Keshet, Aviv and Huang, Wujie and Gillen, Jonathon and Gommers, Ralf and Ketterle, Wolfgang, Physical Review Letters **106** 010402 (2011)

⁴⁹ Y.R. Lee, T.T. Wang, T.M. Rvachov, J.H. Choi, W. Ketterle, and M.-S. Heo, Phys. Rev. A **87**, 043629 (2013)

⁵⁰ Mark J. H. Ku, Ariel T. Sommer, Lawrence W. Cheuk,

Martin W. Zwierlein, Science **335**, 563 (2012).